Larval dispersal of scamp (*Mycteroperca phenax*) in the waters off the southeastern United States: Connectivity within and between the Gulf of Mexico and Atlantic Ocean

SEDAR68-SID-02

28 September 2019

This information is distributed solely for the purpose of pre-dissemination peer review. It does not represent and should not be construed to represent any agency determination or policy.

Please cite this document as:

Brothers, J.R., M. Karnauskas, C.B. Paris, and K.W. Shertzer. 2019. Larval dispersal of scamp (*Mycteroperca phenax*) in the waters off the southeastern United States: Connectivity within and between the Gulf of Mexico and Atlantic Ocean. SEDAR68-SID-02. SEDAR, North Charleston, SC. 35 pp.

Larval dispersal of scamp (*Mycteroperca phenax*) in the waters off the southeastern United States: Connectivity within and between the Gulf of Mexico and Atlantic Ocean

J. R. Brothers[1], M. Karnauskas[2], C.B. Paris[3], and K.W. Shertzer[1]

[1]Southeast Fisheries Science Center

101 Pivers Island Road,

Beaufort, NC 28516

[2]Southeast Fisheries Science Center

Sustainable Fisheries Division

75 Virginia Beach Drive

Miami, FL 33149

[3]University of Miami

Rosenstiel School of Marine and Atmospheric Science

Division of Applied Marine Physics

4600 Rickenbacker Causeway

Miami, FL 33149

Introduction

Connectivity among marine fish populations not only arises through the movements of juveniles and adults, but also through larval dispersal facilitated by ocean currents. Consequently, disparate populations may be connected even when adults display high site fidelity. Indeed, for reef-associated species with long pelagic larval duration (PLD) such as scamp (*Mycteroperca phenax*) and other grouper, larval dispersal may be the dominant mechanism of connectivity among otherwise spatially distinct segments of the stock. Therefore, when determining stock boundaries for the purposes of assessment, it can be useful to evaluate how larval biology and reproductive ecology combine with oceanographic circulation to influence spatial patterns of larval transport and recruitment.

To investigate these questions for scamp, we first combined literature review and data analysis to assess critical elements of scamp larval biology as well as the timing and location of spawning. Then, we used this information to parameterize an individual based biophysical model that tracks simulated larvae in time and space as they move through the ocean.

In particular, we examined whether oceanographic factors are likely to facilitate dispersal of scamp larvae to distant regions, or conversely to favor self-recruitment (a spatial pattern characterized by larvae settling in the vicinity of where they originated). Furthermore, we assessed the regional source and sink dynamics of scamp recruitment patterns, with a specific focus on connectivity between the Gulf of Mexico and the southwestern North Atlantic Ocean. To do this, we used the open source Connectivity Modeling System (CMS; Paris *et al*., 2013), which is specifically designed to study complex larval migrations and has been used previously to estimate the recruitment dynamics and larval transport of reef fish (Karnauskas *et al*., 2013; Gruss *et al*., 2014; Karnauskas *et al*., 2017) and other marine organisms (Kough *et al*., 2013; Le Corre *et al*., 2018).

Methods

Biophysical modeling framework

To conduct the simulations we used the Connectivity Modeling System (CMS) and released a total of 1,715,543 particles (i.e. virtual larvae) from expected spawning areas throughout the northern Gulf of Mexico and southwestern North Atlantic Ocean (see *Spawning location* below). CMS uses the output from hydrodynamic models to advect the simulated larvae and track their movements through time and space. In addition, CMS includes optional modules that facilitate the realistic estimation of larval movements by simulating observed biological phenomena such as egg buoyancy, vertical larval migration, and tidal stream transport (Paris *et al*, 2017).

Ocean velocity fields

We used ocean velocity, temperature, and salinity fields estimated by the South Atlantic Bight and Gulf of Mexico (SABGOM) hydrodynamic model. The details of this model have been described in detail elsewhere (Hyun and He, 2010; Xue *et al*, 2013; Xue *et al*, 2015), but briefly, its domain covers the entire region of interest with a horizontal spatial resolution of

approximately 5 km, and vertically it includes 36 terrain-following layers. We used the output from a seven year (2004-2010) hindcast that was validated against satellite observed sea surface height and surface chlorophyll, as well as *in situ* observations of ocean temperature, salinity, dissolved inorganic nitrogen, and coastal sea level (Xue *et al,* 2013).

Initial conditions of the biological model

To parameterize the biological traits associated with simulated scamp larvae we used a combination of literature review and data analysis. We conducted two sets of simulations that differed in the number of particles released at each location, as described below.

Spawning time

We defined the spawning season for scamp, and therefore, the timing of particle releases in CMS, by analyzing the seasonality of the available reproductive histology data for scamp caught in the Gulf of Mexico (1972-2017) and Atlantic Ocean (1976-2018). These data include 7,409 reproductive samples with associated dates, 955 of which were females within approximately 24 hours of spawning (i.e. hydrated oocytes). From these data, we calculated the 2.5% and 97.5% quantiles of the reported catch dates of all spawning female scamp (Figure 1). In accordance with this analysis, we released particles every other day between day of year 70 and 180 (approximately early March through the end of June). A more detailed description of these reproductive data are provided in Appendix 1.

Furthermore, we scaled the number of particles released on each day to be proportional to the probability of spawning, as predicted by a binomial generalized additive model (GAM) (Figure1). The model predicts a high probability of scamp spawning from March through May, with the highest probability at the end of April. Covariates included in this GAM were average bottom depth at catch location, change in bottom depth at catch location, day of year, year, and whether the sample came from a fishery dependent or fishery independent source. We also considered longitude and latitude as covariates, but they were ultimately excluded from the final model. See Appendix 1 for more details on this model.

The results of these analyses are consistent with previous reports of the scamp spawning season that describe peak spawning as March through May (Harris *et al,* 2002; Farmer *et al,* 2017; Lombardi-Carlson *et al,* 2012).

Spawning location

For our simulations, we generated a grid of release locations spaced at ten kilometer intervals throughout the northern Gulf of Mexico and southwestern North Atlantic Ocean (Figure 2). We based the spatial extent of the locations on where scamp have been observed during fishery independent visual surveys, but only released particles at locations with a bottom depth between 34.09 and 94.19 meters. We calculated this depth range as the 2.5% and 97.5% quantiles of the bottom depths at the catch locations of all spawning female scamp (Appendix 1).

For the first of two simulations, we released particles uniformly across all locations, and only changed the number of particles based on the timing of the release. That is, on any given day, the same number of particles was released from each location. While this does not a realistically reflect the biology of the species, it decouples the effects of oceanographic transport from the effects of spatial variation in spawning stock biomass, and therefore allows us to investigate how oceanographic considerations alone influence recruitment patterns. For example, the uniform simulation identifies spawning regions from which ocean circulation patterns promote high recruitment success, as well as spawning areas from which ocean currents facilitate connectivity via larval dispersal. It does not, however, provide realistic estimates of the magnitude of recruitment or connectivity because it does not account for the spatial distribution of spawning biomass.

Therefore, to more realistically approximate the recruitment patterns of scamp, we conducted a second simulation, for which we scaled the number of particles released at each location such that it is proportional to the probability of finding a spawning female at that location (Figure 3). Because this approach accounts for the spatial distribution of both scamp abundance and scamp spawning it provides insight into the relative number of recruits that each spawning area contributes to particular settlement regions and the entire population. As a result, it identifies the relative influence of different spawning and settlement areas, and more realistically estimates the magnitude of larval connectivity between regions.

For this second simulation we used a multi-step process to scale the number of particles released at each location. First, we used data from five fishery independent visual surveys that span the northern Gulf of Mexico and southwestern North Atlantic Ocean (4 video surveys and 1 diver survey; Appendix 1, Figure S2) to predict scamp abundance at each of the particle release locations. We did this with a delta-GAM approach that uses two different GAMs: a binomial GAM submodel that predicts the probability of scamp presence, and a Gaussian GAM submodel that predicts scamp abundance when present (Appendix 1). The product of the predictions from these two submodels provides the predicted scamp abundance at each location (Figure S3). Both models used the same set of covariates, which included average bottom depth at the survey location, change in bottom depth around the survey location, longitude, latitude, percent substrate, maximum relief, the year the data were collected, and which survey program the data came from. See Appendix 1 for more details on each of these models.

Next, for each release location we multiplied this predicted scamp abundance by the probability of catching a spawning female, when a scamp is caught. We calculated this value using the previously described spawning GAM. This provides the overall probability of a spawning female being present at each location (Figure 3), and we scaled the number of particles released at each location so that it was proportional to this value. See appendix 1 for more detail on these calculations.

The results of these analyses are consistent with previous reports of scamp spawning habitats and locations that described spawning on high relief shelf edge reefs at depths between 50 and 100 meters (Coleman *et al*, 2011; Farmer *et al*, 2017; Harris *et al*, 2002).

Release groups

For computational efficiency, we did not release particles from each location on every day. Instead, as previously described we released particles every other day during the spawning season. Furthermore, we randomly assigned each release location to one of four groups (Figure 2), and released particles from locations in each group on a different set of days (Figure 1). For example one set of locations released particles on days of year 70, 78, 86, etc., and another set of locations released particles on days of year 72, 80, 88, etc. In this way, particles were released every other day, but each location only released particles once every 8 days. Therefore, only one fourth of the locations released particles on any given release day. This approach reduces the total number of overall particles required, but still allows for extensive temporal and spatial coverage.

Spawning depth, egg buoyancy, and vertical distribution of larvae

The simulated depth distributions of particles in the first few days can have significant effects on the ultimate dispersal patterns (Mullon *et al,* 2002). Therefore, we released particles 10 meters above the sea floor, which is consistent with the 1-15 meter range in which scamp courtship behavior has been observed (Gilmore and Jones, 1992; Schobernd and Sedberry, 2009). In addition, we used the buoyancy module in CMS, which applies the physical properties of particles to simulate their sinking or floating and realistically approximate the vertical movement of eggs (Paris *et al,* 2017). These initial vertical movements are defined according to Stoke's Law, which relates vertical velocity to the diameter and density of the particle, along with the density and viscosity of the water. The latter two variables are calculated directly from the oceanographic data for the location of the particle. The diameter of particles was defined using the reported size range for scamp eggs (Bullock and Smith, 1991), but because density values for scamp eggs were not available, we used those reported for red grouper eggs (*Epinephelus morio*; Colin *et al,* 1996). In addition, CMS allows for some variation in the specification of the size and density parameters by incorporating these values as a statistical distribution rather than as a fixed point estimate (Table 1).

After two days, which is the approximate time that grouper eggs typically hatch into larvae (Roberts and Schleider, 1983; Colin *et al,* 1996), simulated particles are subject to vertical migration with depths determined probabilistically from empirical data (Table 2). We calculated the vertical distribution of larvae from icthyoplankton surveys that use Multiple Opening and Closing and Environmental Sensing System (MOCNESS; for a description of sampling see Appendix 1 in Karnauskas *et al,* 2013). Because grouper larvae are rare in the samples and hard to identify to species, we used all Epinephelinae larvae caught during the scamp spawning season (N = 72). This included 54 larvae caught during winter SEAMAP surveys (February and March; G. Zapfe, unpublished data) and 18 larvae caught in spring surveys (May) that are independent from SEAMAP (T. Gerard, unpublished data).

Settlement

We specified the settlement competency period as 33 to 52 days. Because data for scamp are not available, we calculated this interval as the 2.5 % and 97.5% quantiles for the ages of

newly settled gag grouper larvae (Figure S4). We used the "digitize" package in R to extract the ages of newly settled gag larvae from published reports of gag settlement in the northeastern Gulf of Mexico (Fitzhugh *et al*, 2005) and the southwestern North Atlantic Ocean (Adamski *et al*, 2012). These values are also consistent with earlier reports of gag and black grouper (*Mycteroperca bonaci*) larval durations from the southwestern North Atlantic (Keener *et al*, 1988).

Little is known about the settlement habitat of scamp, so we analyzed data for age 0 and age 1 scamp caught in the northeastern Gulf of Mexico (N = 44; L. Lombardi-Carlson, unpublished data; T. MacDonald, unpublished data). Because young scamp were predominantly caught at depths less than 30 meters (Figure S5), we used this as a boundary for suitable settlement habitat. We extracted the 0 and 30 meter isobaths from the global 30 arc-second bathymetry grid available from GEBCO (General Bathymetric Chart of the Oceans; www.gebco.net) and defined suitable settlement habitat as all areas between these isobaths in the northern Gulf of Mexico and southwestern North Atlantic Ocean. In addition, the settlement habitat was divided into 119 similarly sized polygons so that simulated particles could be tracked from source to settlement location. Successful settlement was defined as those particles that reached any of these settlement areas during the competency period, given the suite of previously described behaviors and attributes.

Other CMS specifications

We used several additional CMS modules designed to simulate larval movements more realistically. We used the turbulence module, which adds a random component to the motion of particles and approximates diffusion (Paris *et al*, 2017). This accounts for sub-grid turbulent processes not resolved by the resolution of the hydrodynamic model. Based on the grid size of SABGOM, and the recommendations from Okubo (1971), we used a horizontal diffusivity value of 20 $m^2 s^{-1}$ and a vertical diffusivity value of 10^{-5} $m^2 s^{-1}$.

Because fish larvae are not passive drifters, but instead can likely avoid being stranded by swimming away from the coast, we also used the "avoid coast" algorithm included in CMS. This module more realistically approximates the movements of fish larvae near coastlines by preventing particles from getting stranded on the land mask. Lastly, we used an additional algorithm in CMS that puts particles back into the ocean if they are transported through the uppermost depth level (i.e. the sea surface).

Results

The first simulation, during which particles were released uniformly across locations, highlighted regions with potential for high spawning or recruitment success and identified potential connectivity pathways. The second simulation, for which the number of particles released at each location was proportional to the probability of scamp spawning at that location, more realistically estimated the recruitment patterns of scamp.

There was a predominant pattern of self-recruitment, with the majority of particles settling in the vicinity of their release location (Figure 4). Similarly, on a larger spatial scale,

particles released from the Atlantic Ocean only settled in the Atlantic Ocean, and particles released in the Gulf of Mexico tended to settle in the Gulf of Mexico (Figure 5). There were however, some particles released from the Gulf of Mexico that successfully settled in the Atlantic Ocean (Figure 6). These particles came from a limited region off the west coast of Florida (Figure 7), and represent on average approximately 8% of the total recruitment to the Atlantic Ocean (Table 3).

These trends remained across all simulation years (2004-2008), but there was some variation. In particular, the specific region along the west Florida shelf that promoted connectivity with the Atlantic Ocean changed slightly across years (Figures S10, S11, S12, and S13). In simulation year 2006 the majority of particles that left the Gulf of Mexico and recruited to the Atlantic Ocean were released south of latitude 26 degrees. By contrast, in simulation year 2007 release locations as far north as latitude 30 degrees sent particles to the Atlantic. In addition, the percent of particles from this region in the Gulf of Mexico that recruited to the Atlantic Ocean and the percent of Atlantic recruits that originated in the Gulf of Mexico both varied across years (Table 3). This indicates that variation in oceanographic conditions influences the magnitude of connectivity between the two regions.

Although the two simulations were largely consistent, there were some notable differences. In particular, the uniform simulation identified the west Florida shelf and the Florida Keys as potential sources of connectivity between the Gulf of Mexico and Atlantic Ocean. Results from the scaled simulation, however, indicated that spawning is unlikely in the Florida Keys, and therefore, connectivity was limited to release locations along the west Florida shelf. In addition, both simulations identified the west Florida shelf, as well as waters off the coasts of Georgia and South Carolina, as recruitment areas that would be favored by ocean circulation. Results from the scaled simulation were similar, but also showed reduced recruitment to the Atlantic coast of Florida. Both simulations highlighted the west Florida shelf, and waters off the coast of Georgia as the areas that oceanographic conditions would promote the greatest spawning success.

Discussion

These results are based on the currently available information about scamp reproductive ecology and larval behavior. The findings may change as new data become available and the individual based model is refined. In particular, there is a clear knowledge gap on the preferred nursery habitat of scamp pre-settlement larvae. Choice of settlement criteria is likely to influence simulation results, and therefore, sensitivity analyses could be used to quantify the effect that the uncertainty in settlement has on our results.

Similarly, there is limited data available to define the vertical distribution of scamp larvae in the water column. Consequently, additional sensitivity analyses would be useful to quantify the effects that the uncertainty in this distribution, as well as the potential for ontogenetic shifts in it, might have on our results.

Another source of uncertainty is the oceanographic fields used during the simulations. We used the output from the SABGOM hydrodynamic model, but other models, such as the Hybrid Coordinate Ocean Model (HYCOM), can also be used. Related work has investigated

how the choice of hydrodynamic model influences the results of CMS simulations. The unpublished work suggests that SABGOM and HYCOM produce similar results in terms of overall connectivity, but that SABGOM tends to transport particles further "downstream" along the Loop Current (i.e. farther south along the west Florida shelf and farther north in the Atlantic). In addition, simulations using HYCOM tend to produce slightly higher rates of self-recruitment than those using SABGOM. Therefore, our results might represent a high-end estimate of the connectivity between the Gulf of Mexico and Atlantic Ocean, but further investigation would help to quantify the uncertainty due to the oceanographic model used.

Although incorporating these considerations may modulate our results, the findings suggest that scamp larvae are likely to recruit to areas close to where they originated. That said, spawning in a limited region along the west Florida shelf, and the associated larval dispersal by ocean currents, results in a small but annually present degree of connectivity between the Gulf of Mexico and Atlantic Ocean. These spawning locations may be important to the resilience of the Atlantic Ocean stock.

Acknowledgements

This report is a preliminary working document that has not completed the internal review process at the Southeast Fisheries Science Center. The scientific results and conclusions, as well as any views and opinions expressed herein, are those of the authors and do not necessarily reflect those of any government agency. In addition, the authors would like to thank the many people who provided data and made this project possible. Nate Bacheler, Jeremiah Blondeau, Matthew Campbell, Chris Gardner, Ted Switzer, and Kevin Thompson provided visual survey data. Linda Lombardi-Carlson, Sue Lowerre-Barbieri, and Tracey Smart provided reproductive histology data. Trika Gerard and Glenn Zapfe provided larval catch data. Linda Lombardi-Carlson and Tim MacDonald provided catch data for young fish. Chuanmin Hu provided the SABGOM data and Ana C. Vaz modified the SABGOM output to allow coupling with CMS.

References

Bacheler, N.M., and Shertzer, K.W. (2015). Estimating relatice abundance and species richness from video surveys of reef fishes. *Fishery Bulletin,* Vol. 113 (1): 15-26.

Bullock, L.H., and Smith, G.B. (1991). Memoirs of the hourglass cruises. Volume VIII (Part II), Seabasses (Pisces: Serranidae). Florida Marine Research Institute, Dept. of Natural Resources. St. Petersburg, Florida.

Campbell, M.D., Pollack, A.G, Gledhill, C.T., Switzer, T.S., and DeVries, D.A. (2015). Comparison of relative abundance indices calculated from two methods of generating video count data. *Fisheries Research,* Vol. 179: 125-133.

Colin, P.L., Koenig, C.C., and Laroche, W.A. (1996). Development from egg to juvenile of the red grouper (*Epinephelus morio*) (Pisces: Serranidae) in the laboratory. In *Biology,*

fisheries and culture of tropical groupers and snappers. Eds. Arreguín-Sánchez, F., Munro, J.L., Balgos M.C., and Pauly, D. pp. 399-414.

Farmer, N.A., Heyman, W.D., Karnauskas, M., *et al.* (2017). Timing and locations of reef fish spawning off the southeastern United States. *PLoS ONE*, Vol. 12 (3): e0172968.

Gilmore, R.G, and Jones, R.S. (1992). Color vartiation and associated behavior in the epinepheline groupers, *Mycteroperca mirolepis* (Goode and Bean) and *M. phenax* Jordan and Swain. *Bulletin of Marine Science*, Vol. 51 (1): 83-103.

Grüss, A., Karnauskas, M., Sagarese, S.R., *et al*. (2014). Use of the Connectivity Modeling System to estimate the larval dispersal, settlement patterns and annual recruitment anomalies due to oceanographic factors of red grouper (*Epinephelus morio*) on the West Florida Shelf. SEDAR42-DW-03. SEDAR, North Charleston, SC. 24 pp.

Harris, P.J., Wyanski, D.M., White, D.B., and Moore, J.L. (2002). Age, growth, and reproduction of scamp *Mycteroperca phenax*, in the southwestern North Atlantic, 1979-1997. *Bulletin of Marine Science,* Vol. 70 (1): 113-132.

Hyun, K.H., He, R. (2010). Coastal upwelling in the South Atlantic Bight: A revisit of the 2003 cold even using long term observations and model hindcast solutions. *Journal of Marine Systems*, Vol. 83: 1-13.

Karnauskas, M., Paris, C.B., Zapfe, G., *et al*. (2013). Use of the Connectivity Modeling System to estimate the movements of gag grouper (*Mycteroperca microlepis*) recruits in the northern Gulf of Mexico. SEDAR33-DW18. SEDAR, North Charleston, SC. 12 pp.

Karnauskas, M., Walter III, J.F., and Paris, C.B. (2017). Use of the Connectivity Modeling System to estimate movements of red snapper (*Lutjanus campechanus*) recruits in the northern Gulf of Mexico. SEDAR52-WP-20. SEDAR, North Charleston, SC. 13 pp.

Kough, A.S., Paris, C.B., and Butler IV, M.J. (2013). Larval Connectivity and the International Management of Fisheries. *PLos ONE*, Vol. 8 (6): e64970.

Le Corre, N., Pepin, P., Han, G. Ma, Z., Snelgrove, P.V.R. (2018) Assessing connectivity patterns among management units of the Newfoundland and Labrador shrimp population. *Fisheries Oceanography*, Vol. 28: 183-202.

Lombardi-Carlson, L.A., Cook, M., Lyon, H., Barnett, B., Bullock, L. (2012). A description of age, growth, and reproductive life history traits of scamps from the northern Gulf of Mexico. *Marine and Coastal Fisheries*, Vol. 4 (1): 129-144.

Marra, G., and Wood, S.N. (2011). Practical variable selection for generalized additive models. *Computational Statistics & Data Analysis*. Vol. 55 (7): 2372-2387.

Mullon, C., Cury, P., and Penven, P. (2002). Evolutionary individual-based model for the recruitment of anchovy (*Engraulis capensis*) in the southern Benguela. *Canadian Journal of Fisheries and Aquatic Sciences*, Vol. 59: 910-922.

Okubo, A. (1971). Oceanic diffusion diagrams. *Deep-Sea Research*, Vol. 19: 789-802.

Paris, C.B., Helgers, J., van Sebille, E., Srinivasan, A. (2013). Connectivity Modeling System: A probabilistic modeling tool for the multi-scale tracking of biotic and abiotic variability in the ocean. *Environmental Modelling & Software*, Vol. 42: 47-54.

Paris, C.B., Vaz, A.C., Helgers, J., Wood, S., Ross, R. (2017). Connectivity Modeling System Users's Guide. CMS v 2.0. University of Miami, Florida.

Roberts, Jr., D.E., and Schlieder, R.A. (1983). Induced sex inversion, maturation, spawning, and embryogeny of the protogynous grouper, *Mycteroperca microlepis*. *Journal of World Mariculture Society*, Vol. 14: 639-649.

Schobernd, C.M., and Sedberry, G.R. (2009). Shelf-edge and upper-slope reef fish assemblages in the South Atlantic Bight: Habitat chaaracteristics, spatial variation and reproductive behavior. *Bulletin of Marine Science*, Vol. 84 (1): 67-92.

Schobernd, Z.H., Bacheler, N.M., and Conn, P.B. (2014). . *Canadian Journal of Fisheries and Aquatic Sciences*, Vol. 71: 464-471.

Xue, Z., He, R., Fennel, K., *et al.* (2013). Modeling ocean circulation and biogeochemical variability in the Gulf of Mexico. *Biogeosciences*, Vol. 10: 7219-7234.

Xue, Z., Zambon, J., Yao, Z., Liu, Y., and He, R. (2015). An integrated ocean circulation, wave, atmosphere, and marine ecosystem prediction system for the South Atlantic Bight and Gulf of Mexico. *Journal of Operational Oceanography*, Vol. 8 (1): 80-91.

Figures

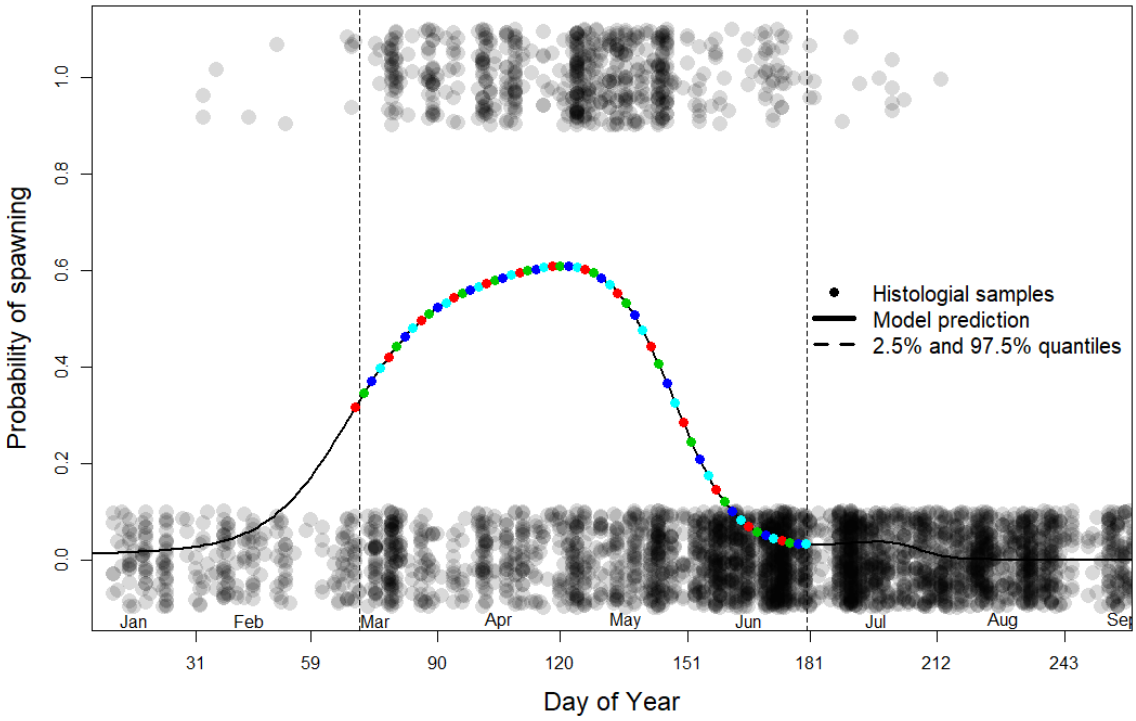

Figure 1. Timing of scamp spawning. A generalized additive model predicts that the probability of scamp spawning (when a scamp is caught) is highest in April and May. The black data points denote the catch day of all available scamp histological samples; the data points along the top indicate females within approximately 24 hours of spawning (i.e. hydrated oocytes) and the data points along the bottom indicate all other scamp histological samples. The vertical dashed lines represent the 2.5% and 97.5% day of year quantiles of spawning females (day of years 70 and 180), which were used to define the spawning season for the simulations. The number of particles released on any given day of year was proportional to the probability of spawning predicted by the model (black line). The colored circles along the model prediction indicate release days (every other day between 70 and 180), with the color denoting the release group (only one quarter of locations had a release on each day).

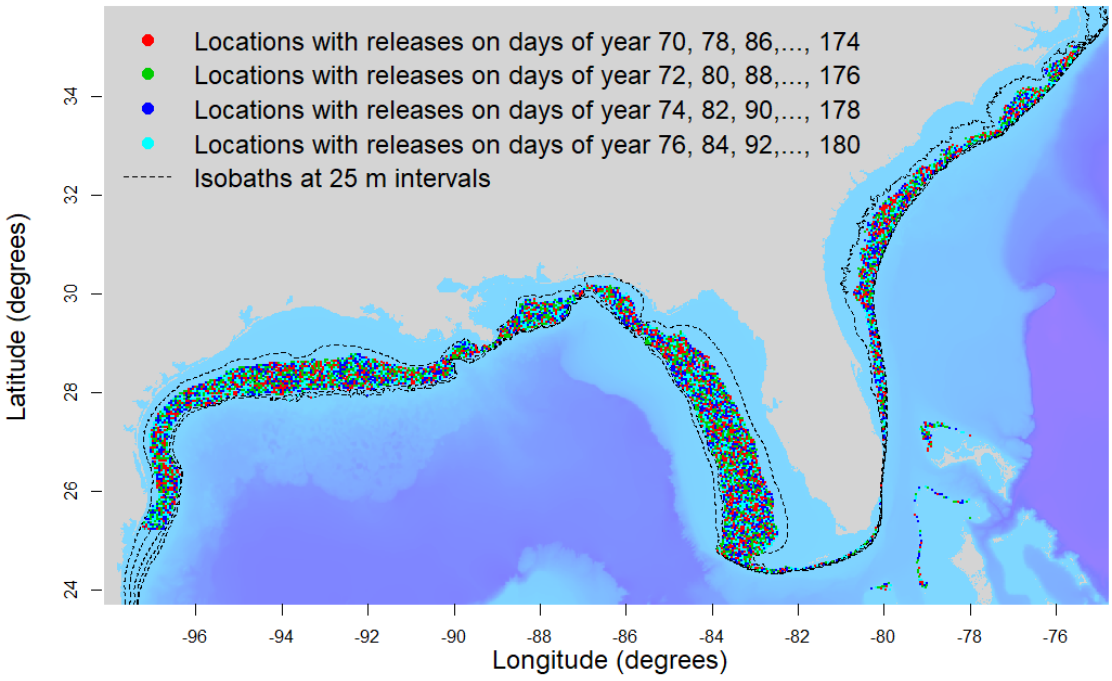

Figure 2. Map of release locations. Release locations were spaced evenly at 10 km increments, throughout the northern Gulf of Mexico and southwestern North Atlantic Ocean. The colors represent the release group. Each location was randomly assigned to one of four release groups so that only one fourth of locations release on any given release day. The spatial extent of the release locations was defined by where visual surveys have looked for scamp and the depth limits (34.19 meters and 94.19 meter) was defined from the depth distribution of spawning female scamp.

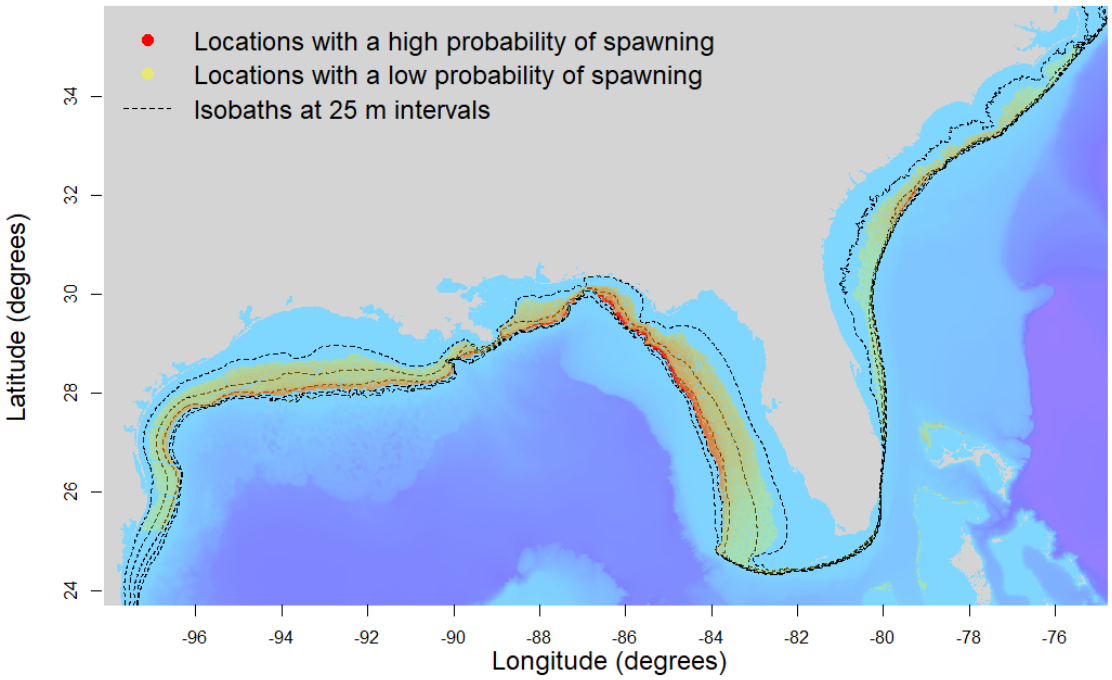

Figure 3. Map of release locations colored by the probability of finding a spawning female scamp. Red indicates a high probability, yellow indicates a low probability. This value was used to scale the number of particles released at each location during the second (scaled) particles release simulation. These probabilities were calculated as the product of three GAM predictions (probability of scamp presence, scamp abundance when present, and probability of catching a spawning female when a scamp is caught).

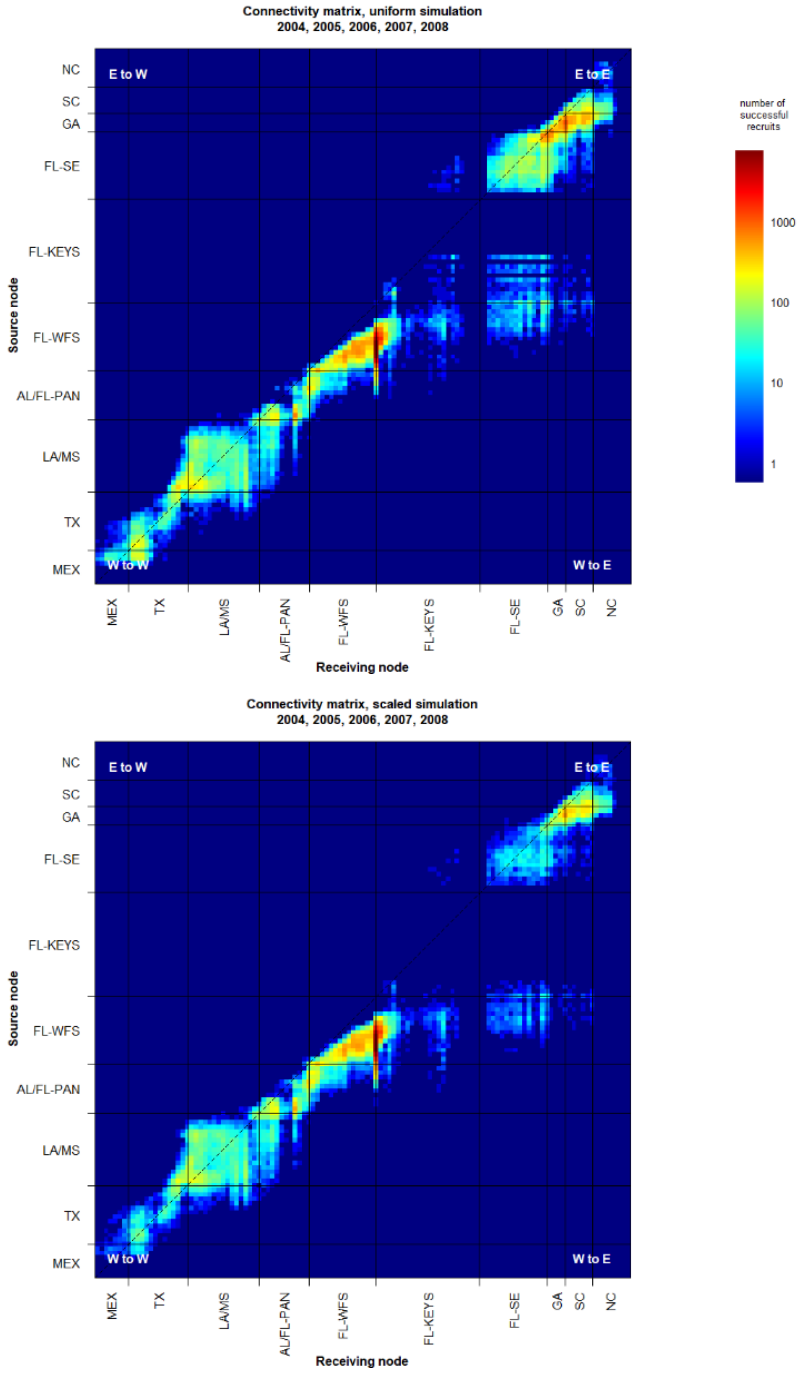

Figure 4. Connectivity matrices for all years (2004-2008) aggregated for the uniform (top) and scaled (bottom) particle release simulations. The y-axis represents where a particle was released and the x-axis indicates where that particle successfully settled. The colors denote the number of successful recruits (on a log scale). The dashed black diagonal line represents the axis of self-recruitment (i.e. a particle settled in the same area that it was released). MEX = Mexico, TX = Texas, LA/MS = Louisiana and Mississippi, AL/FL-PAN = Alabama and the Florida Panhandle, FL-WFS = the west Florida shelf, FL-KEYS = the Florida Keys, FL-SE = the east coast of Florida, GA = Georgia, SC = South Carolina, NC = North Carolina. See supplemental figures each year individually.

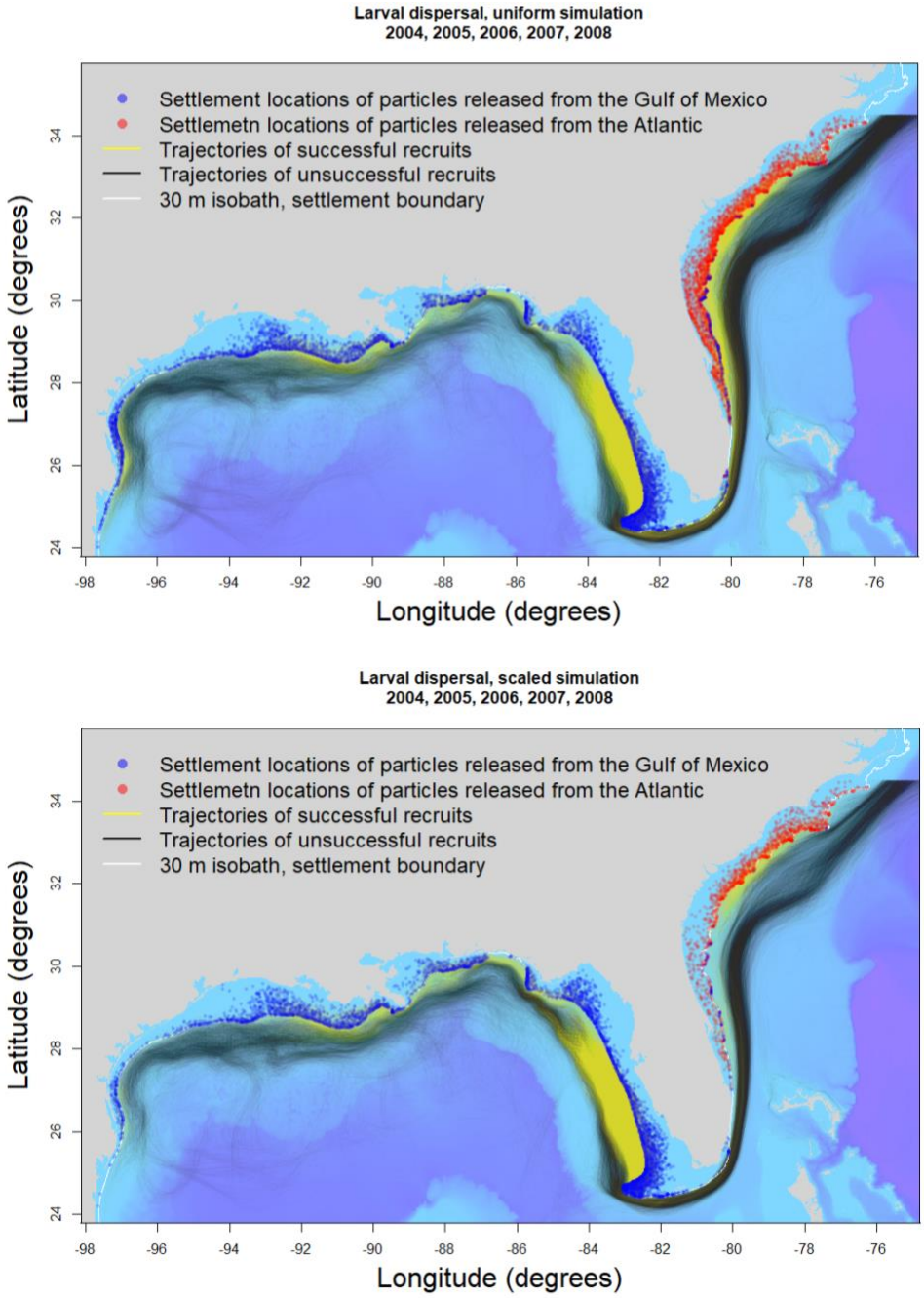

Figure 5. Map of settlement locations for all years (2004-2008) aggregated for the uniform (top) and scaled (bottom) particle release simulations. Although particles tended to settle within the region from which they were released, some particles left the Gulf of Mexico and successfully settled in the Atlantic Ocean (blue dots in the Atlantic Ocean). For clarity, only 10% of the total particles are shown. See supplemental figures for the same maps of each year individually for the uniform (Figure S11) and scaled (Figure S12) simulations.

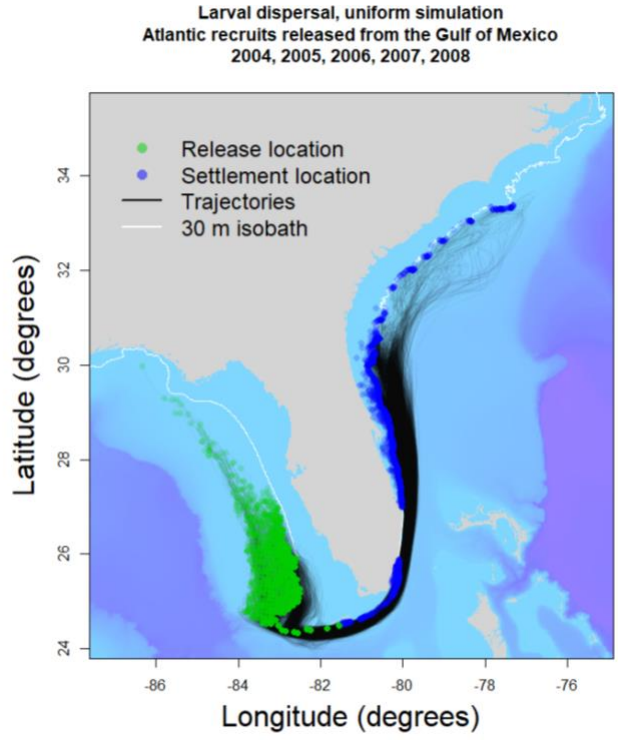

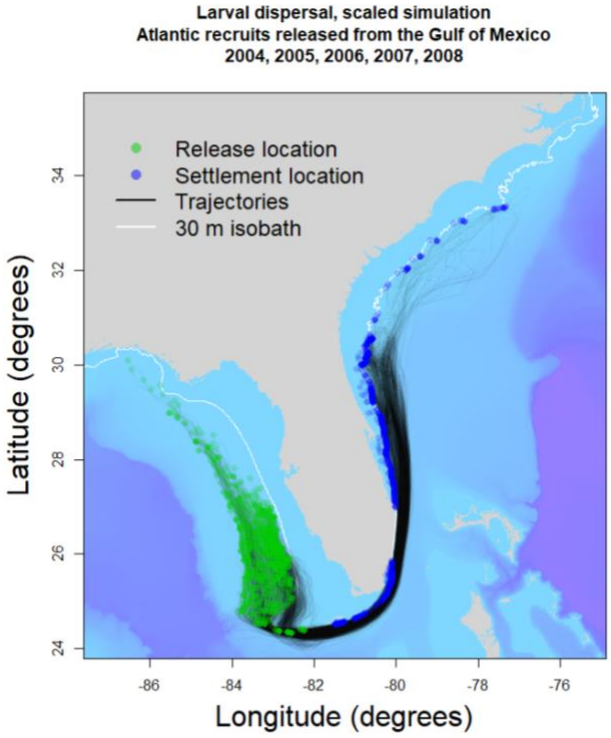

Figure 6. Map of release locations for only those particles that were released in the Gulf of Mexico and settled in the Atlantic Ocean; all years (2004-2008) aggregated for the uniform (top) and scaled (bottom) particle release simulations. See supplemental figures for each year individually.

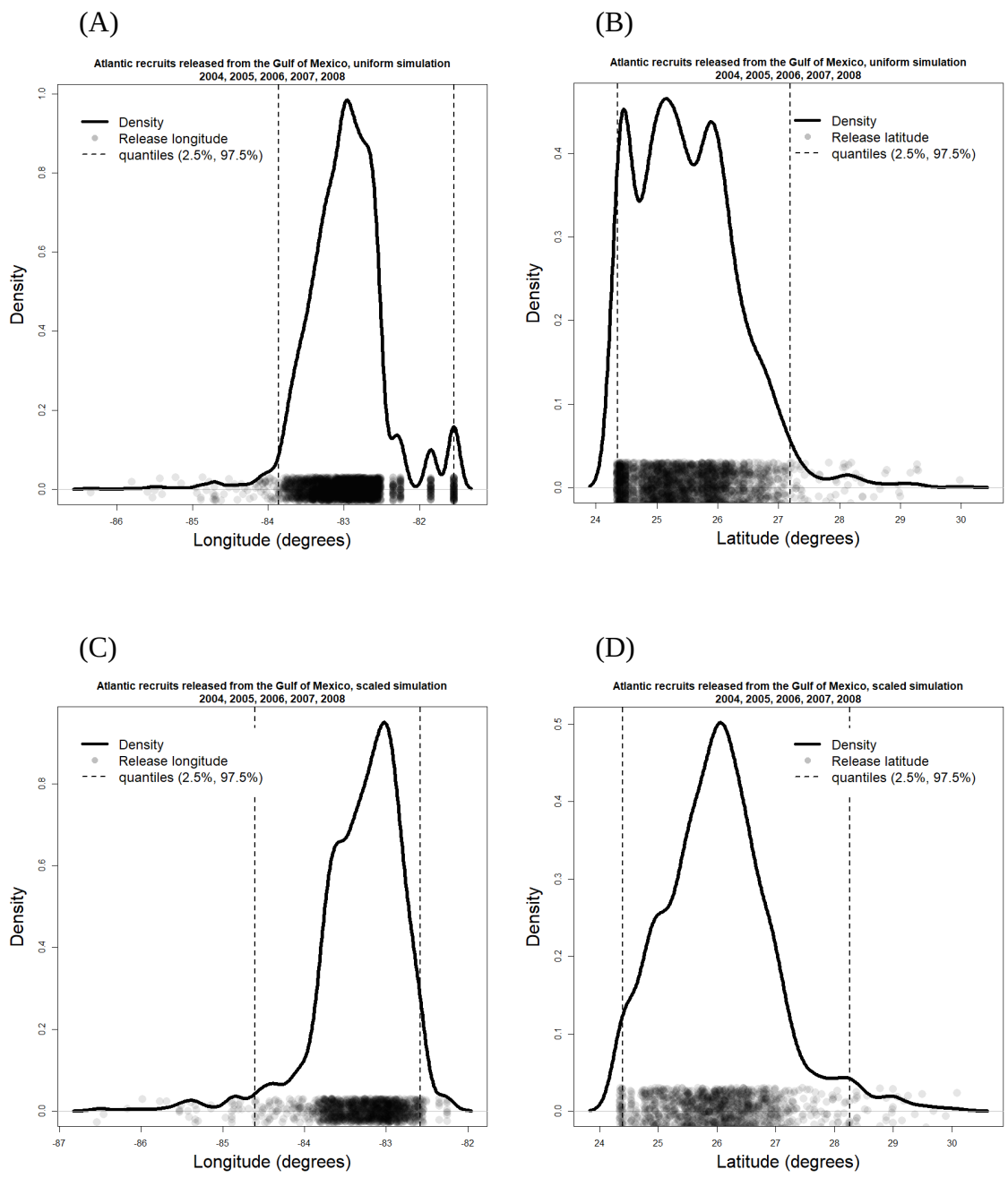

Figure 7. Latitude and longitude distributions of the release locations for only those particles that originated in the Gulf of Mexico but recruited to the Atlantic Ocean; all years (2004-2008) aggregated for the uniform (A and B) and scaled (C and D) particle release simulations. See supplemental figures for the same maps of each year individually for the uniform (Figure S15) and scaled (Figure S16) simulations.

Tables

Table 1. Specifications of the variability in the density and size of simulated particles.

Percentage of particles in each category	25%	50%	25%
Minimum density (kg m^{-3})	1018.7	1019.7	1020.7
Maximum density (kg m^{-3})	1019.7	1020.7	1021.7
Minimum particle diameter (mm)	0.75	0.87	0.99
Maximum particle diameter (mm)	0.99	1.11	1.23

Table 2. Vertical distribution applied to simulated scamp larvae.

Depth bin (meters)	Percentage of particles
0-20	60
20-40	32
40-60	08
60-80	0
80-100	0

Table 3. Percent connectivity between the Gulf of Mexico and Atlantic Ocean. For the uniform simulation we calculated the percent of successful particles originating in the eastern Gulf of Mexico (e.g. west Florida shelf and Florida Keys) that settled anywhere in the Atlantic Ocean. For the scaled simulation, we calculated this same percentage, but also calculated the percent of recruits to the Atlantic Ocean that originated from anywhere in the Gulf of Mexico

	Scaled simulation		Uniform simulation
Year	% ATL from GoM	% E-GoM to ATL	% E-GoM to ATL
All	7.6	1.6	3.9
2004	7.7	0.9	2.7
2005	3.4	0.7	2.4
2006	10.7	1.9	5.0
2007	9.1	2.6	3.7
2008	7.1	2.6	5.7

Appendix – Data sets and models used to parameterize the biological model

Reproductive histology data

We used three sources of reproductive histology data for scamp in the northern Gulf of Mexico and southwestern North Atlantic Ocean. Together, these sources provided data for 7,465 histological samples including 1,448 females with hydrated oocytes (Figure S1). The National Marine Fisheries Service (NMFS) laboratory in Panama City, Florida provided data for 2,718 scamp histological samples. These samples are overwhelmingly from fish caught in the Gulf of Mexico, are largely fishery dependent samples, and include 796 spawning females. Florida Fish and Wildlife Research Institute (FWRI) provided data for 11 spawning females that were caught in the Gulf of Mexico during fishery independent surveys. South Carolina Department of Natural Resources (SC-DNR) provided data for 4,736 histology samples. These samples were all caught in the southwestern North Atlantic Ocean, are from a combination of fishery dependent (N = 2,521) and fishery independent (N = 2,215) sources, and include 641 spawning females.

To define the spawning season of scamp, we used data from all spawning females that had an associated catch date, and calculated the 2.5% and 97.5% quantiles for the catch day of year (70.85 and 180.15, respectively). Therefore, we only released particles between day of year 70 and 180.

To define the depth range at which we released particles we used data from all spawning females that had an associated catch location. First, we calculated the mean bottom depth in a grid cell around the catch location. To do this, we used the 3 arc-second resolution bathymetry grid produced by the Coastal Relief Model (CRM, www.ngdc.noaa.gov/mgg/coastal/crm.html) and calculated the mean depth at all CRM grid locations within 0.01 degrees longitude and latitude of each catch location. Then, we calculated the 2.5% and 97.5% quantiles for these mean depths (34.09 and 94.19 meters, respectively) and only released particles at release locations with mean depths in this range.

Spawning GAM

With this histology data, we used the "mgcv" package in R to develop a binomial generalized additive model (GAM) to predict the probability that a caught scamp would be a female with hydrated oocytes (i.e. a female within 24 hours of spawning). The full suite of covariates considered for this spawning GAM included longitude, latitude, average bottom depth around the catch location, change in bottom depth around the catch location, day of year, year, and whether the sample came from a fishery dependent or fishery independent source.

As described above, we used the 3 arc-second resolution bathymetry grid produced by the Coastal Relief Model to calculate the average bottom depth around each catch location. We used the same approach to calculate the change in bottom depth around each catch location. For this, however, we calculated the maximum difference in bottom depth across all CRM grid locations within 0.025 degrees longitude and latitude of the catch location. This metric approximates the bathymetric slope and provides some information about where the location is relative to the continental shelf break. That is, a low value for the change in depth suggests a catch location is on the continental shelf, but a high value suggests that a catch location is at or near the shelf

break. We tried various spatial resolutions, but the 0.01 degree value for average depth and 0.025 degree value for change in depth resulted in the best model fits.

For this, and all subsequent GAMs, we conducted variable selection with the "select = TRUE" argument built into the "gam()" function in the "mgcv" R package. This method adds an additional smoothing penalty that allows spurious covariates to be eliminated from the model, and it is the recommended approach to variable selection for GAMs (Mara and Wood, 2011). For this spawning GAM, longitude and latitude were eliminated from the model, and the final set of covariates included average depth, change in depth, day of year, year (as a factor), and fishery status. The model explained 44.6% of the deviance in whether a sample was a spawning female and had an adjusted r^2 of 0.402.

We calculated the marginal effect of day of year (Figure 1) by setting all other covariates to a constant value. Continuous variables (e.g. bottom depth) were set to the median value of all spawning female data and categorical variables (e.g. fishery status) were set to the most frequent level among all spawning female data. We took a similar approach to predict the probability of spawning at each release locations (Figure 2). For this, however, we used both the average depth around the release location and the change in depth around the release location while the other three covariates were set to the median or mode.

Visual survey data

To define the spatial distribution of scamp we used data from five fishery independent visual surveys that sample in the northern Gulf of Mexico or southwestern North Atlantic Ocean (Figure S2). This includes four video surveys (FWRI, NMFS-MS, NMFS-PC, SEFIS) and one diver survey (RVC). Although each survey focuses primarily on a different region, there is considerable spatial overlap between them. All three video surveys that sample in the Gulf of Mexico overlap (FWRI, NMFS-MS, NMFS-PC). The diver survey (RVC), which samples in the Florida Keys overlaps with the FWRI video survey. The FWRI video survey also has limited sampling along the east coast of Florida, and therefore overlaps with the video survey in the southwestern North Atlantic Ocean (SEFIS). We only used data collected between years 2011 and 2017 because not all surveys sampled outside of this range.

Three of the four video survey programs quantified scamp abundance using the max N metric (FWRI, NMFS-MS, NMFS-PC), which is the highest number of individuals observed at any single time point during an entire video (Campbell *et al*, 2015). This is sometimes also referred to as mincount because it represents the minimum estimate of how many fish are present at the site. The fourth video survey (SEFIS), however, uses the sum count (or the associated mean count) metric. This is the sum (or mean) of the number of fish observed on 41 frames throughout the video (Schobernd *et al*, 2014). Although both metrics have merits, in order to compare the data across surveys we used the individual frame counts from the SEFIS data to calculate an estimated max N as the maximum number of scamp observed on a single frame. Although this is not a true max N, because SEFIS videos are only read for 41 frames rather than the full video, evidence suggests that analysis of limited frames can closely approximate analysis of the entire video (Bacheler and Shertzer, 2015).

Scamp spatial distribution delta GAM

We predicted the spatial distribution of scamp by analyzing these visual survey data with a two-step delta GAM approach. First, we developed a binomial GAM submodel to predict the probability of scamp presence. Next, we used only those survey data that observed scamp to develop an additional GAM submodel that predicts scamp abundance when present. Then, we estimated the overall abundance of scamp at each release location as the product of these two predictions (Figure S3).

Both of these submodels used the same set of covariates, which included all variables that overlap across all five surveys. These are longitude, latitude, average depth (from the CRM model as described above), change in depth (from the CRM model as described above), year, percent substrate, relief, and which survey program the data came from. To standardize covariates across surveys we calculated percent substrate as the percent of the bottom that is covered by rock, hard coral, or soft coral. We also sorted relief into three levels; we categorized locations with a maximum relief less 0.3 meters as "low relief," locations with a maximum relief between 0.3 and 1.0 meters as "moderate relief," and locations with a maximum relief greater than 1.0 meter as "high relief."

Variable selection did not eliminate any covariates for either GAM, so both final submodels included the entire suite of covariates that overlap across the surveys. The binomial GAM submodel that predicted probability of scamp presence explained 26.2% of the deviance in whether a survey observed scamp and had an adjusted r^2 of 0.246.

For the positive count submodel we considered various error distributions, including Gaussian with a fourth root or log transformation, Tweedie, Quasipoisson, Gamma, and Negative Binomial. The Gaussian error distribution with fourth root transformed scamp counts performed the best (selected based on AIC value) and explained 27% of the deviance in survey counts (when scamp were observed) and had an adjusted r^2 of 0.259.

Particle release scaling

For each year (2004-2010) we released particles every other day between day of year 70 and 180 (56 release days per year; Figure 1). In total, we released particles at 6,198 locations throughout the Gulf of Mexico and southwestern Atlantic Ocean (Figure 2). One fourth of these locations released particles on any given release day. For each release event (a combination of release day and release location) the number of particles was determined in two steps. First, we used the marginal day of year effect from the spawning GAM to distribute particles across the release days according to the probability of spawning on that day. For the uniform simulation we stopped here, and for each release day distributed these particles evenly across all locations. In this way, each location released the same number of particles but simulations still realistically approximated the scamp spawning season.

For the second simulation, however, we also considered the spatial distribution of scamp abundance and spawning. For each release day, we took the total number of particles released and distributed them across the release locations using the results of the spatial analyses described above. For each release location we first predicted the probability of scamp presence using the longitude, latitude, bottom depth, and change in bottom depth at that location. Second,

we predicted scamp abundance when present at each release location using the same covariates. Third we predicted the probability of finding a spawning female if a scamp is caught at a given release location using the bottom depth and change in bottom depth at each location (we did not use the longitude and latitude in this prediction because these covariates were not included in the final spawning GAM). Finally, we calculated the overall probability of finding a spawning female scamp at each location as the product of these three predictions (Figure 3), and for each release day we used these values to distribute the number of particles released across the release locations.

Supplemental Figures

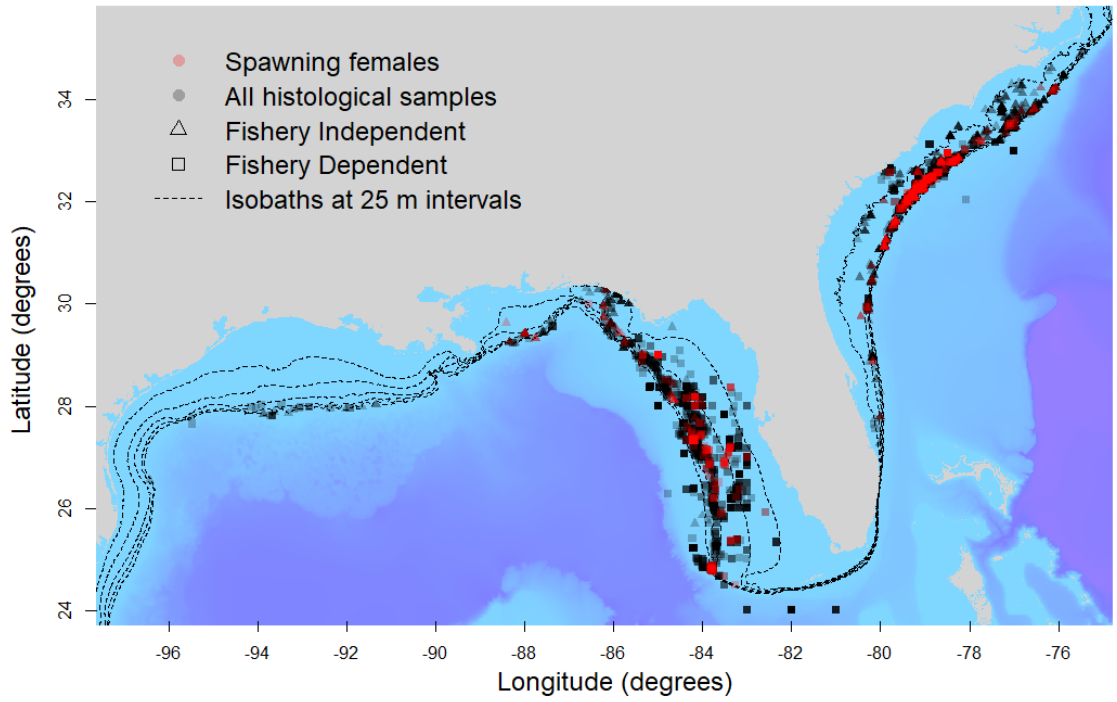

Figure S1: A map showing the locations of all scamp histological samples. Red data points represent the catch locations for female scamp with hydrated oocytes (i.e. within approximately 24 hours of spawning), and black data points represent the catch locations of all other scamp histological samples. Triangles denote samples form fishery independent sources, while squares indicate samples from fishery dependent sources.

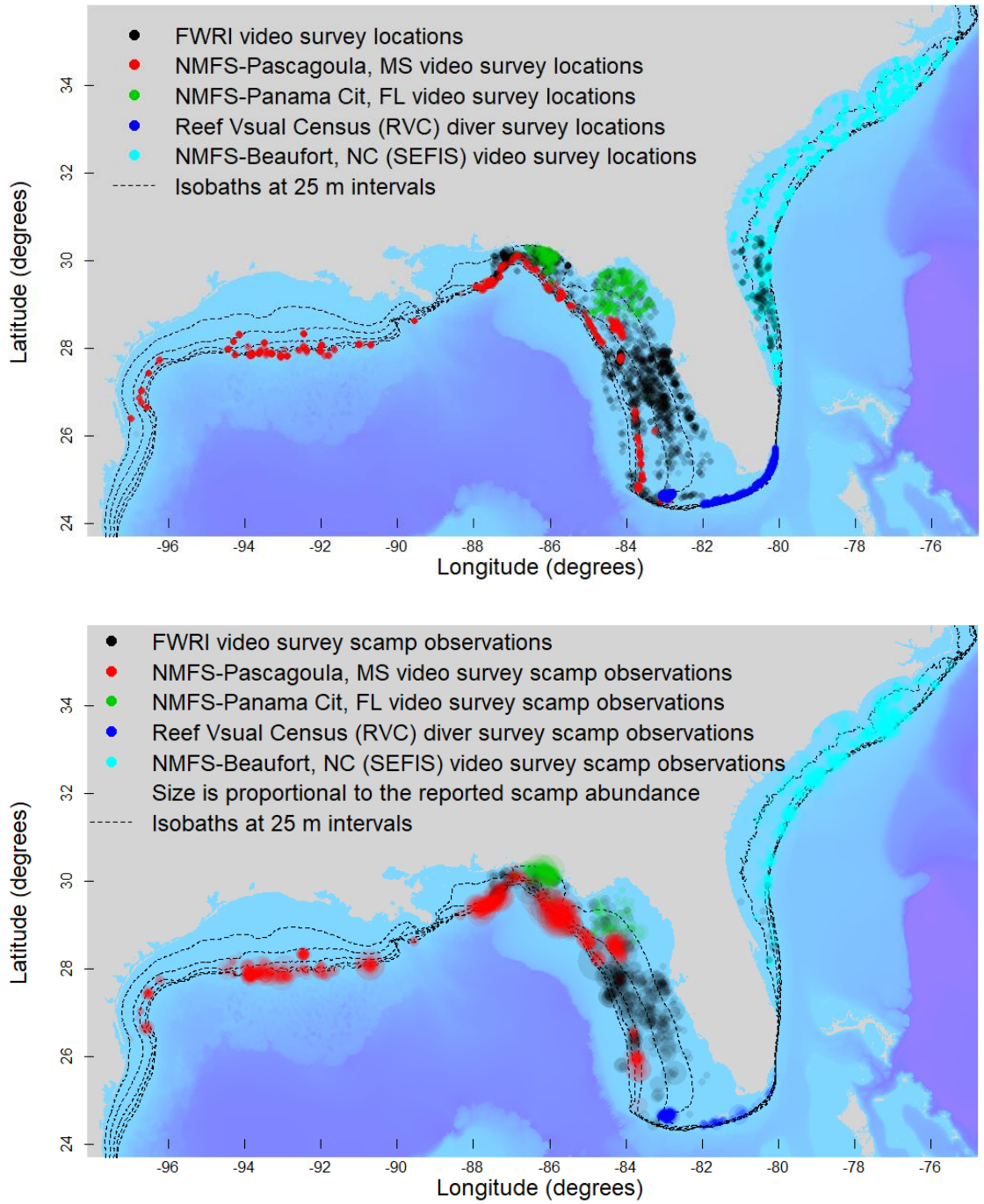

Figure S2: A map showing the locations of all visual survey locations colored by survey program (top), and a map showing only those survey locations that observed scamp (bottom). For the bottom map the size of each data point is proportional to the reported abundance of scamp during that survey. The video survey conducted by the NMFS laboratory in Pascagoula, MS, samples near the continental shelf break throughout the northern Gulf of Mexico. The video survey conducted by the NMFS laboratory in Panama City, Florida samples relatively shallow locations in the northeastern Gulf of Mexico. The video survey conducted by FWRI samples a wide depth

range along the west Florida shelf, with limited sampling along the eastern coast of Florida. The video survey conducted by the NMFS laboratory in Beaufort, NC samples a wide depth range throughout the southwestern Atlantic Ocean. The Reef Visual Census (RVC) is a multi-agency diver survey that samples in the Dry Tortugas and Florida Keys.

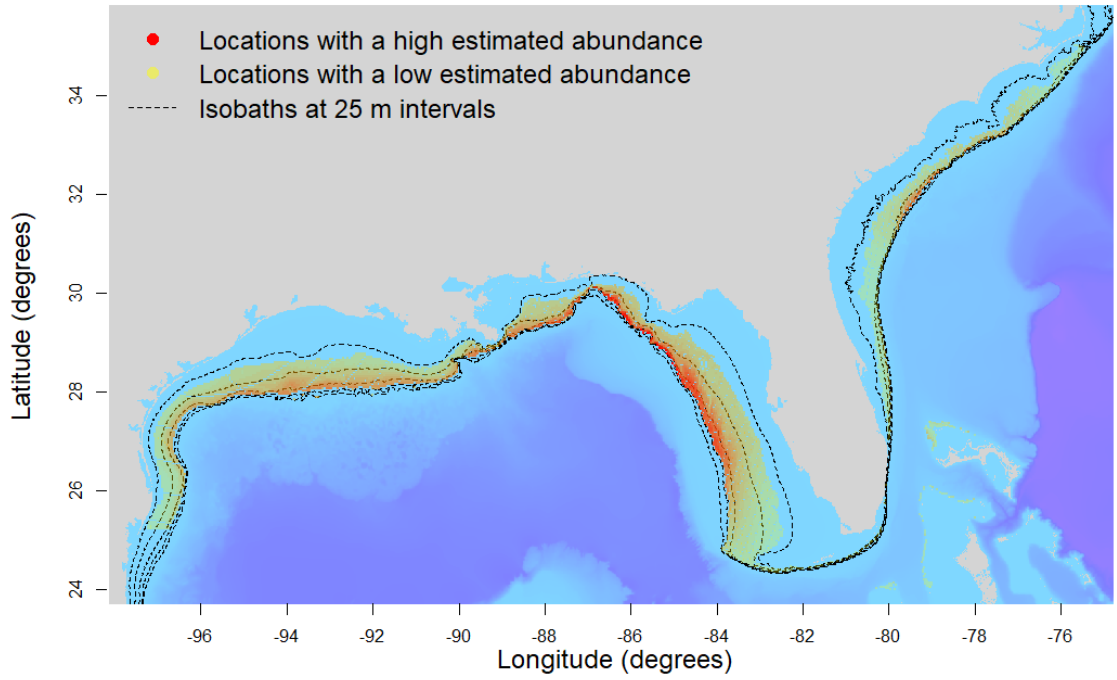

Figure S3: The estimated scamp abundance at each release location. This was calculated as the product of the two visual survey models included in the delta GAM approach used: the binomial GAM that predicts the probability of scamp presence, and the Gaussian GAM that predicts scamp abundance when present.

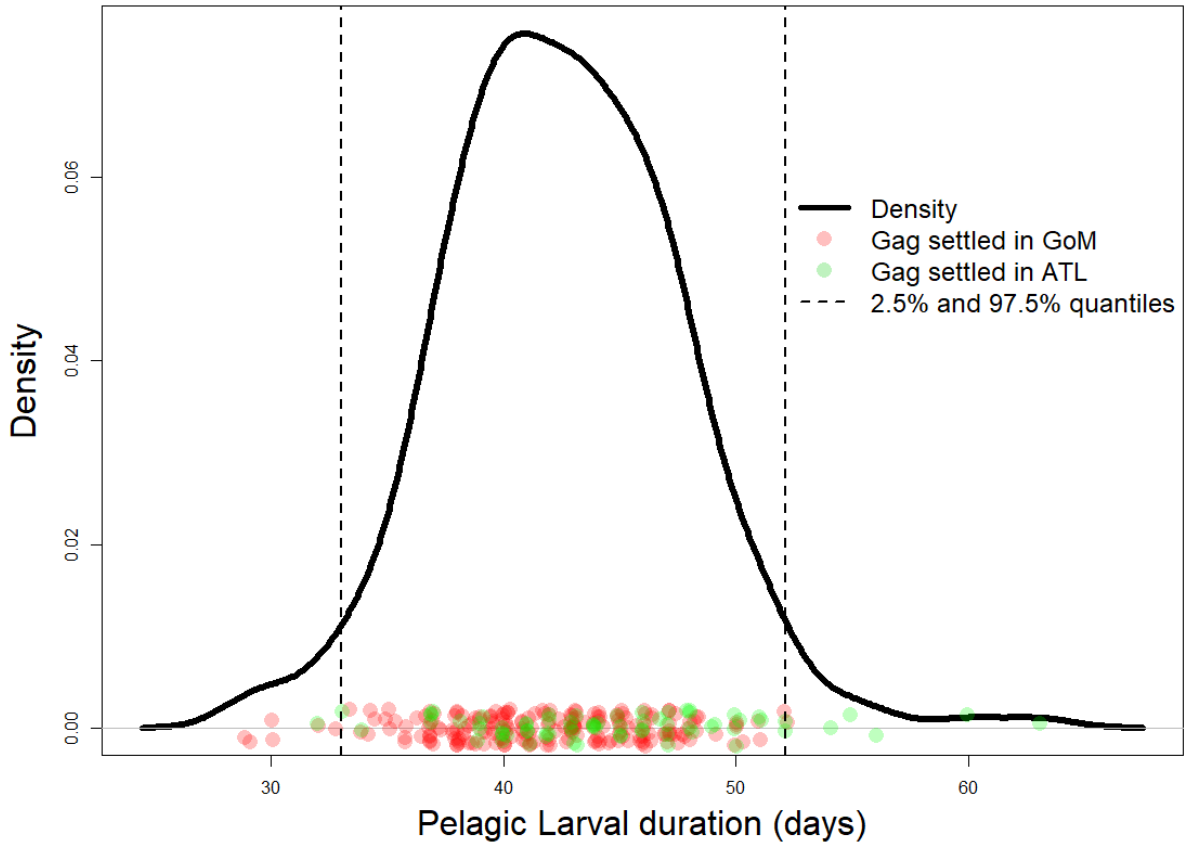

Figure S4: A density plot showing the ages of newly settled gag larvae. Red data points represent the pelagic larval duration (PLD, in days) of gag larvae in the Gulf of Mexico. Green data points represent the PLD of gag larvae in the Atlantic. Data digitized from Fitzhugh *et al.* (2005; Gulf of Mexico) and Adamski *et al.* (2012; Atlantic).

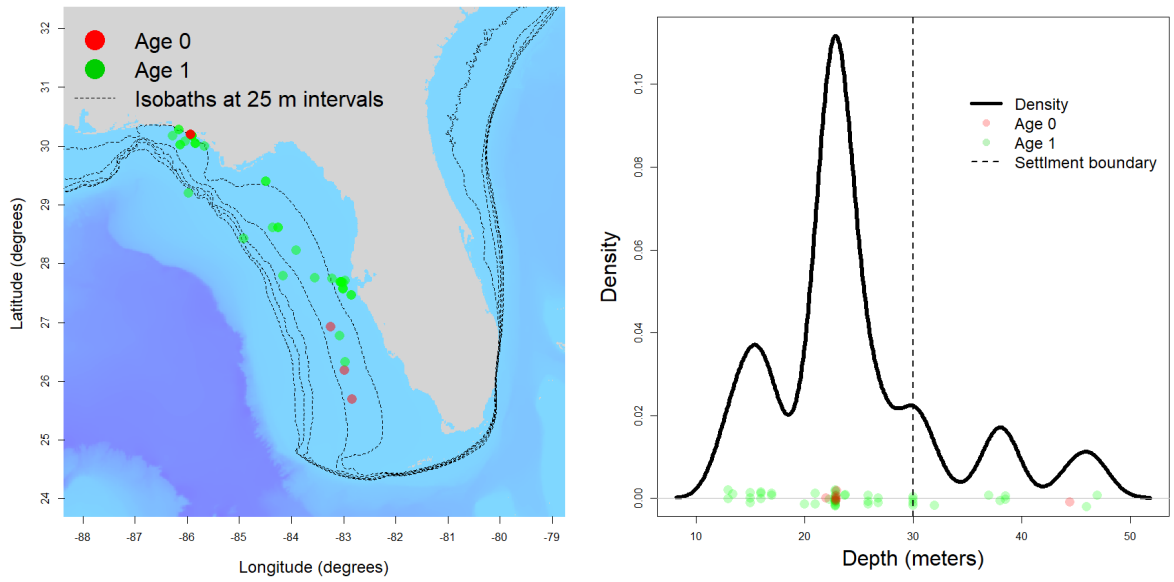

Figure S5: A map showing the catch locations of age 0 and age 1 scamp (left) and a plot showing the depth distribution at the catch locations of these fish (right). Red data points indicate the catch location or depth of age 0 scamp. Green data points indicate the catch location or depth of age 1 scamp. The solid black line (right) represents the depth distribution of young scamp, and the dashed vertical black lines denote the 2.5% and 97.5% quantiles of the depths at which young scamp were caught.

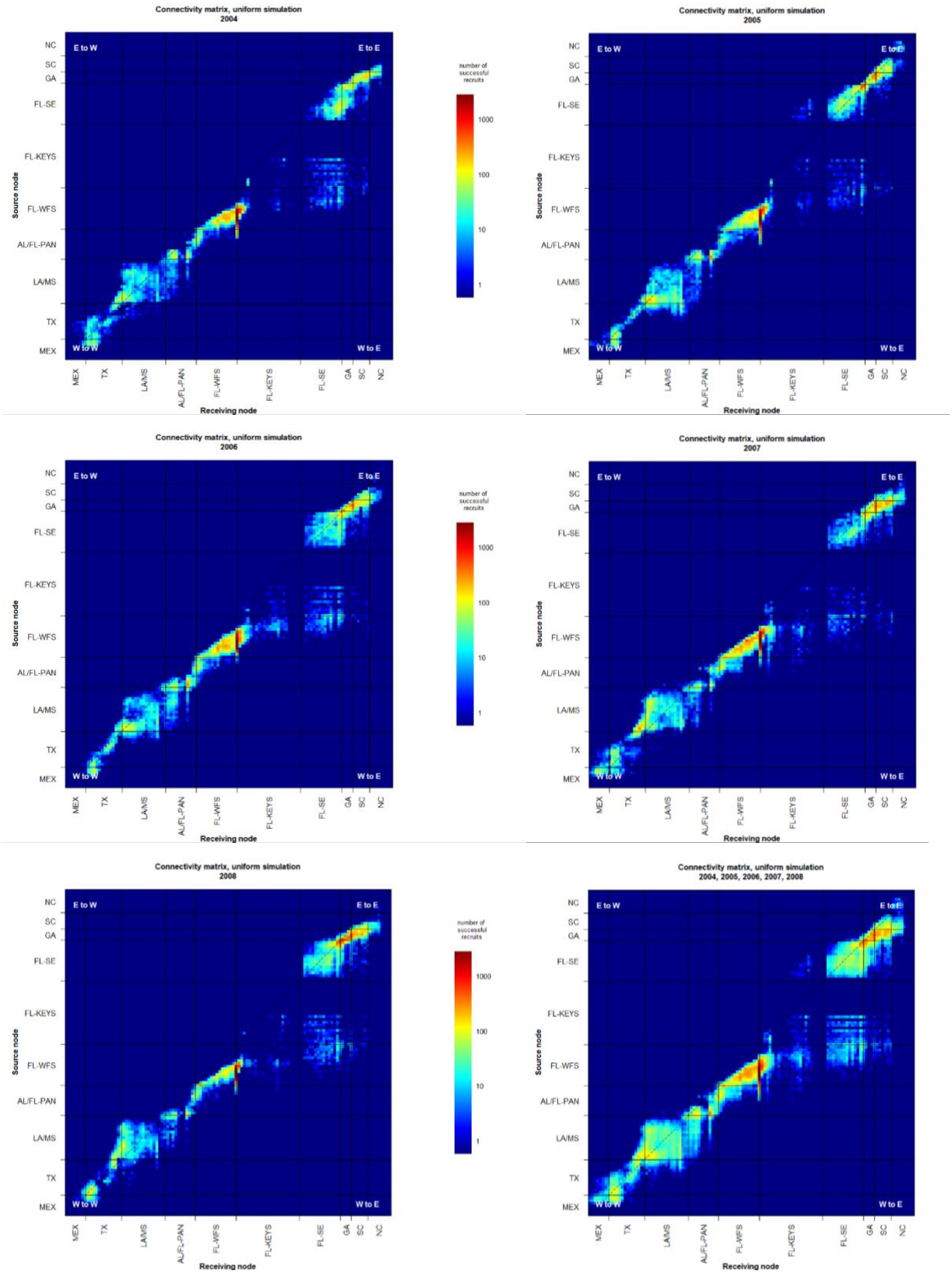

Figure S6. Connectivity matrices for each individual year of the uniform particle release simulation.

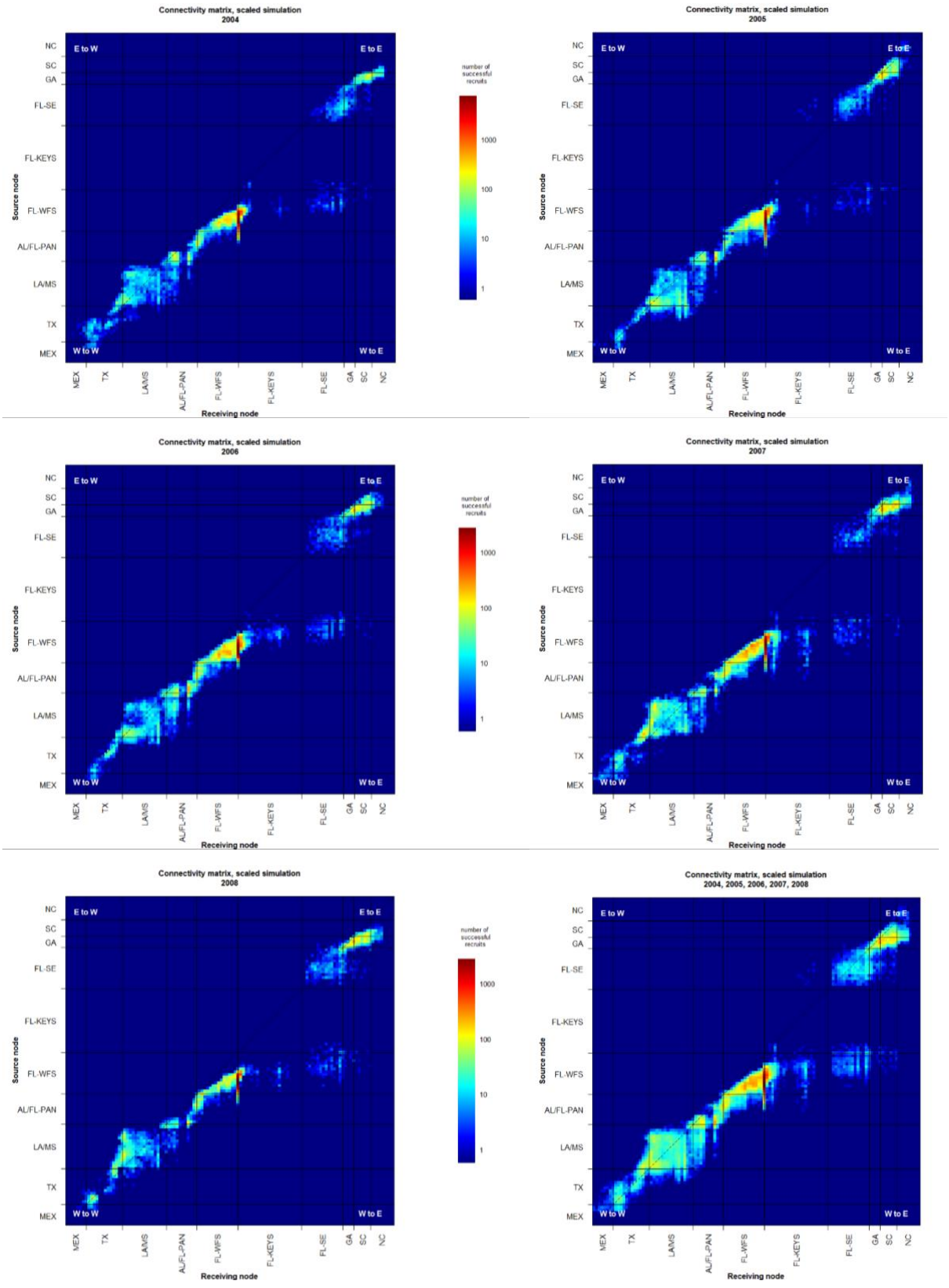

Figure S7. Connectivity matrices for each individual year of the scaled particle release simulation.

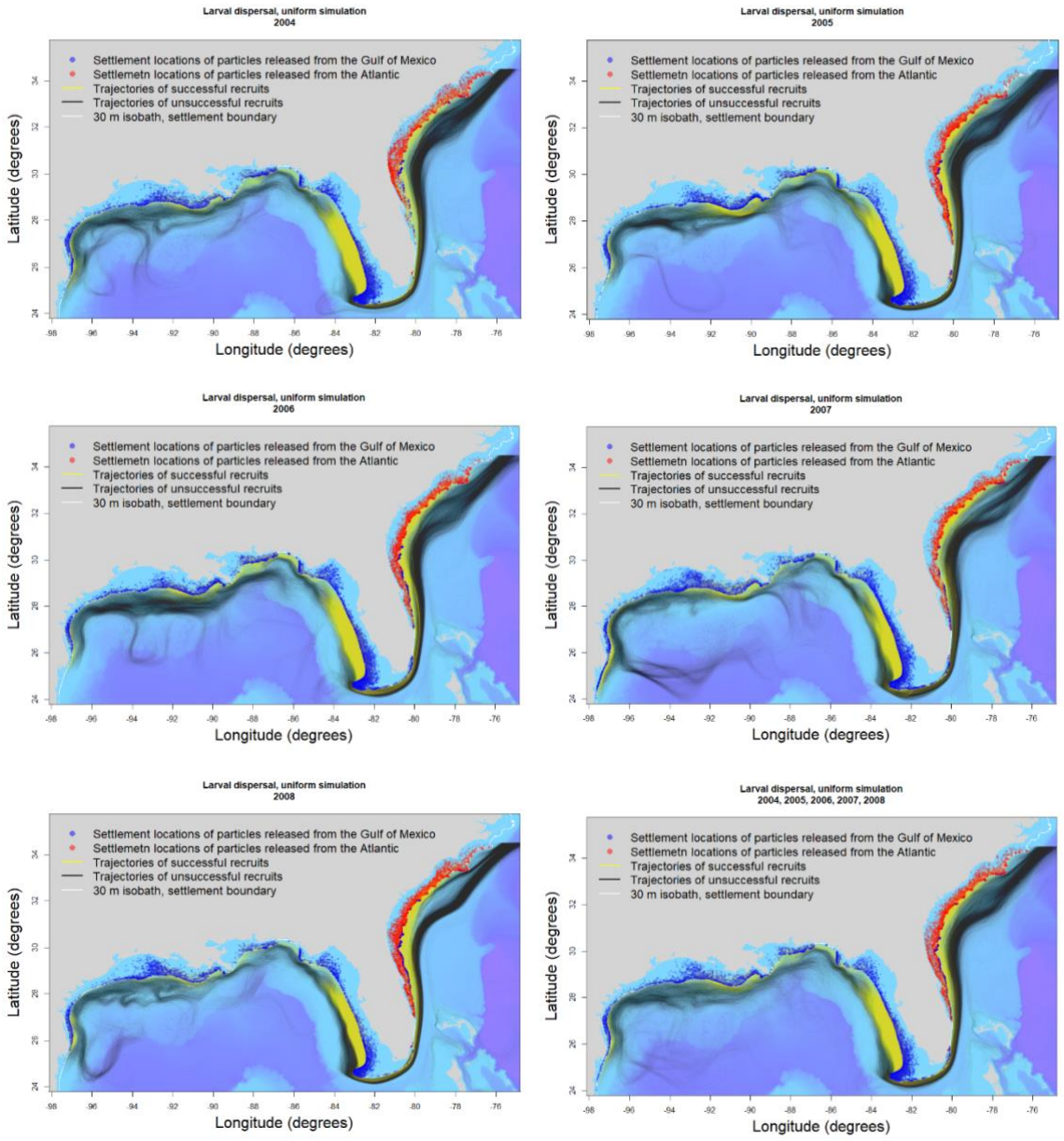

Figure S8. Map of settlement locations for individual years of the uniform particle release simulation.

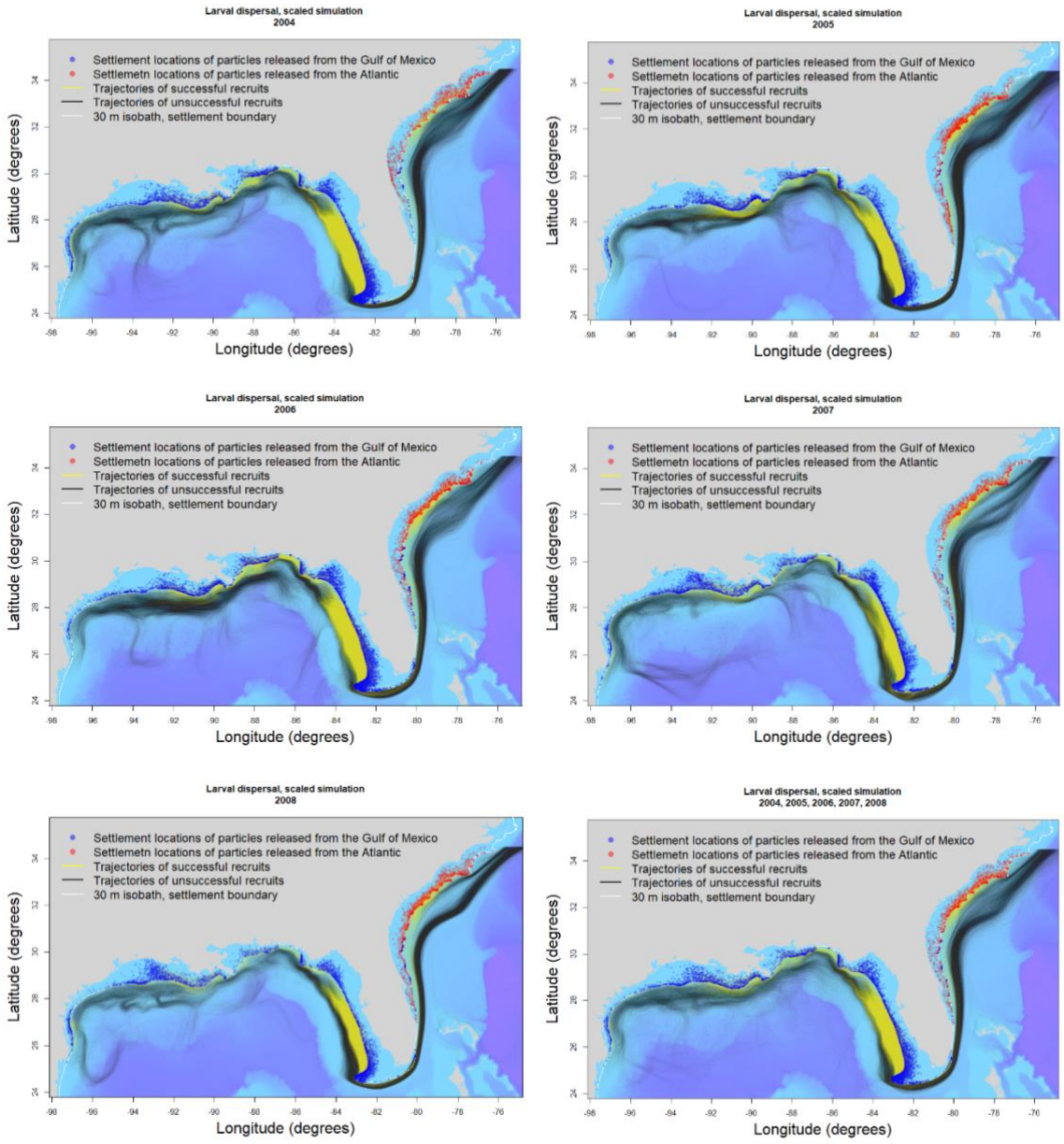

Figure S9. Map of settlement locations for individual years of the scaled particle release simulation.

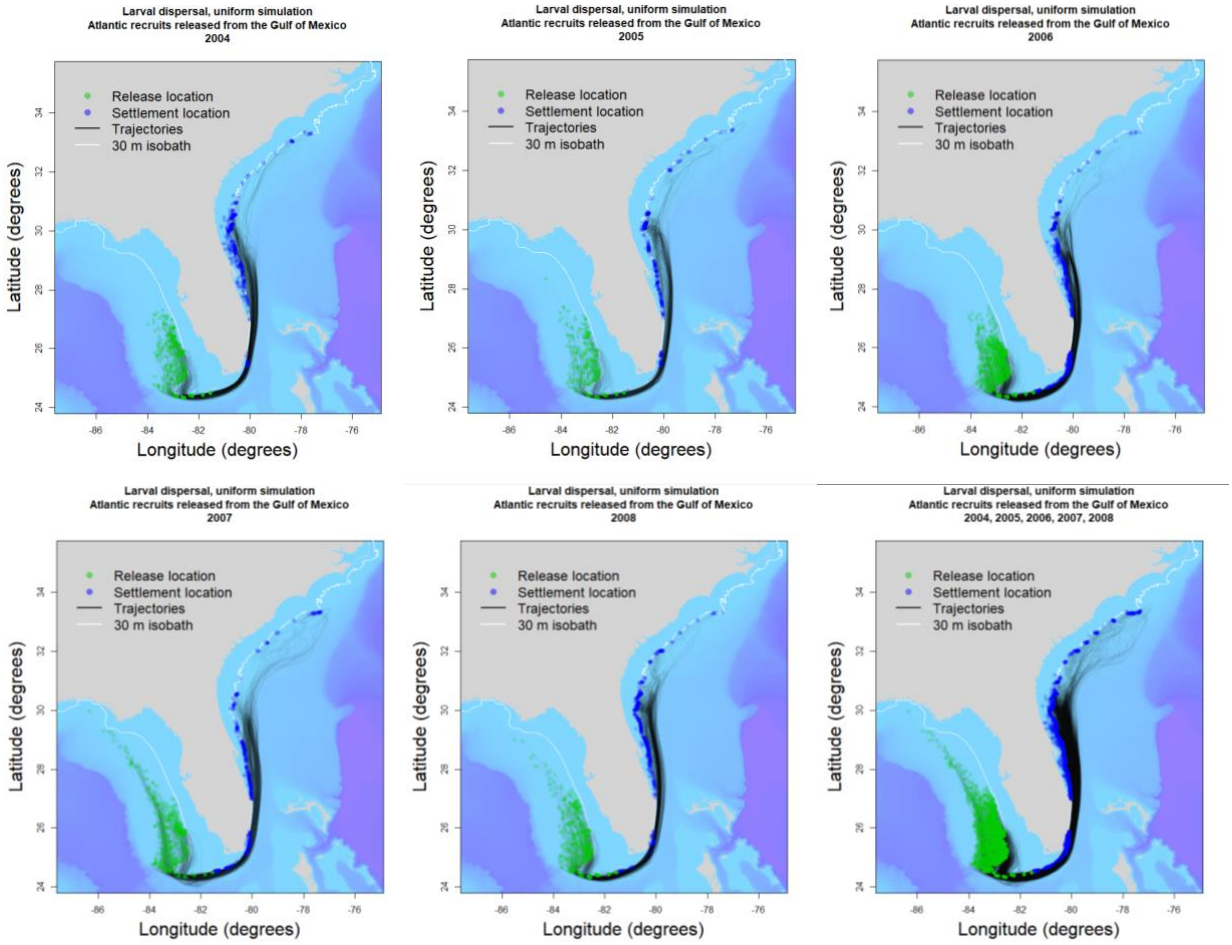

Figure S10. Map of release location of Gulf of Mexico to Atlantic Recruits for individual years of the uniform particle release simulation.

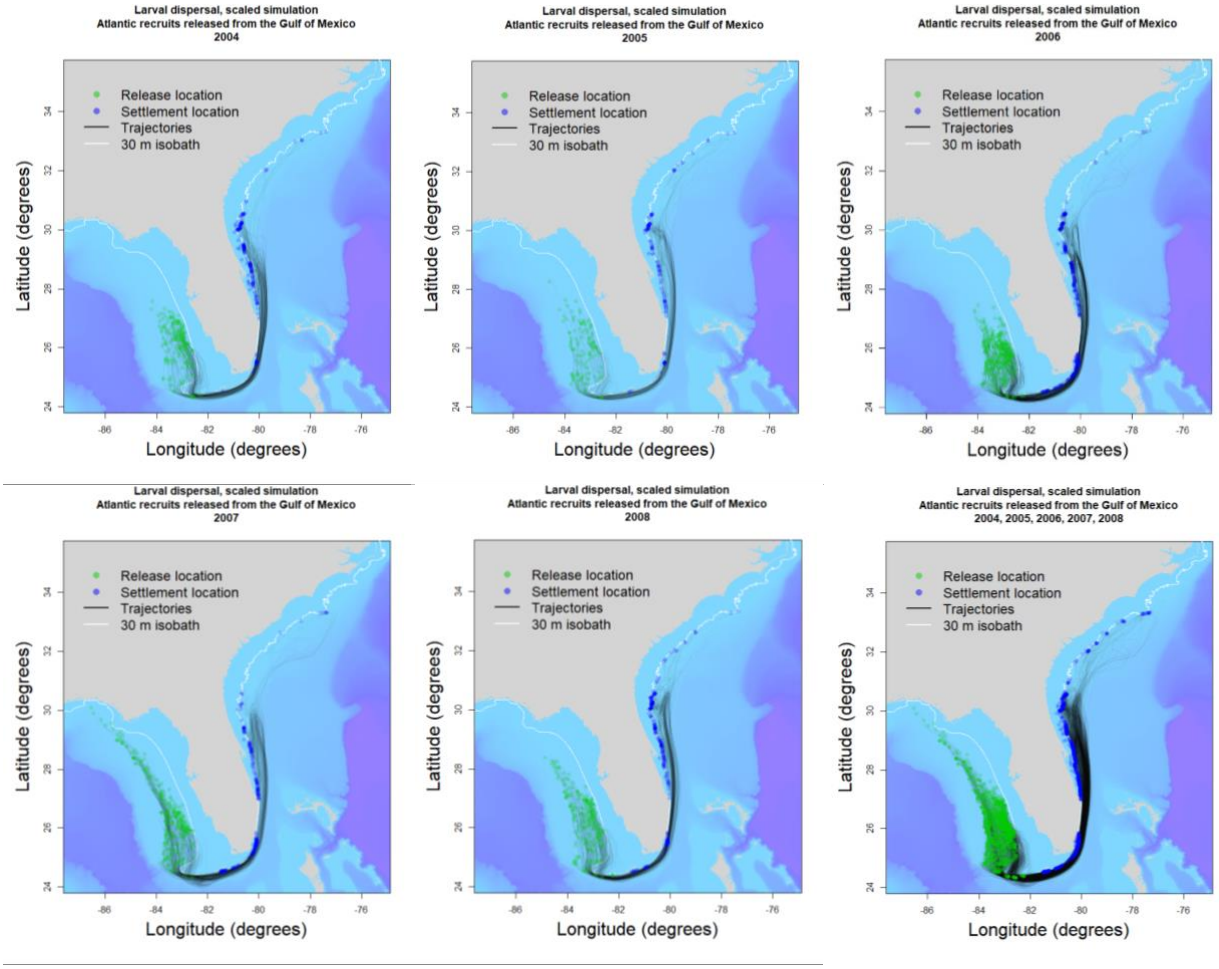

Figure S11. Map of release locations of Gulf of Mexico to Atlantic Recruits for individual years of the scaled particle release simulation.

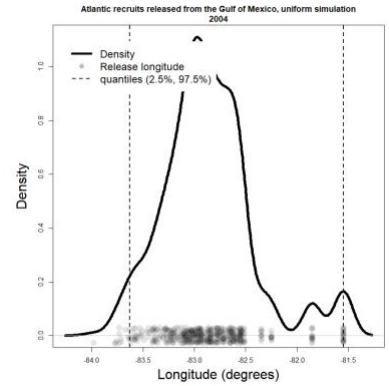
Atlantic recruits released from the Gulf of Mexico, uniform simulation
2004
Density
Release longitude
quantiles (2.5%, 97.5%)
Density
Longitude (degrees)

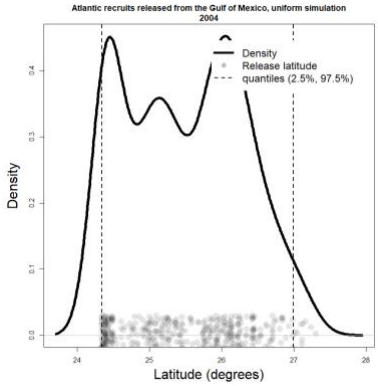
Atlantic recruits released from the Gulf of Mexico, uniform simulation
2004
Density
Release latitude
quantiles (2.5%, 97.5%)
Density
Latitude (degrees)

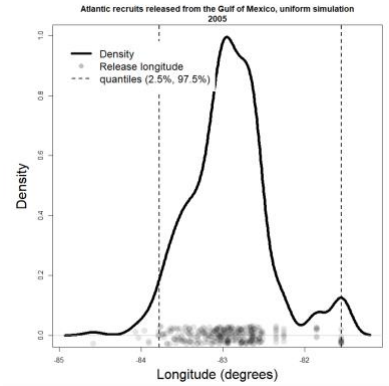
Atlantic recruits released from the Gulf of Mexico, uniform simulation
2005
Density
Release longitude
quantiles (2.5%, 97.5%)
Density
Longitude (degrees)

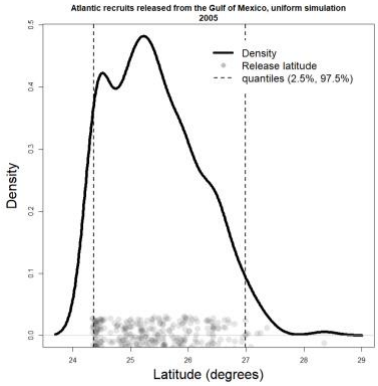
Atlantic recruits released from the Gulf of Mexico, uniform simulation
2005
Density
Release latitude
quantiles (2.5%, 97.5%)
Density
Latitude (degrees)

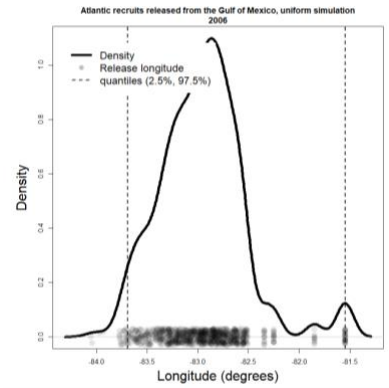
Atlantic recruits released from the Gulf of Mexico, uniform simulation
2006
Density
Release longitude
quantiles (2.5%, 97.5%)
Density
Longitude (degrees)

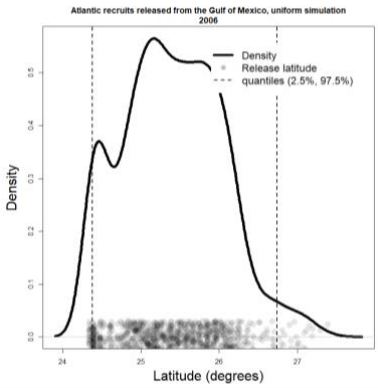
Atlantic recruits released from the Gulf of Mexico, uniform simulation
2006
Density
Release latitude
quantiles (2.5%, 97.5%)
Density
Latitude (degrees)

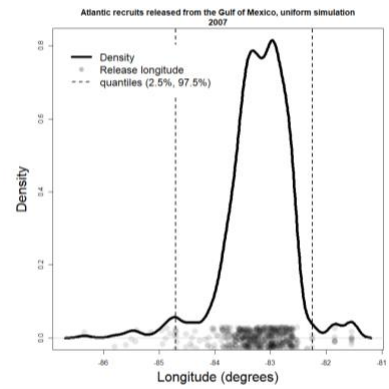
Atlantic recruits released from the Gulf of Mexico, uniform simulation
2007
Density
Release longitude
quantiles (2.5%, 97.5%)
Density
Longitude (degrees)

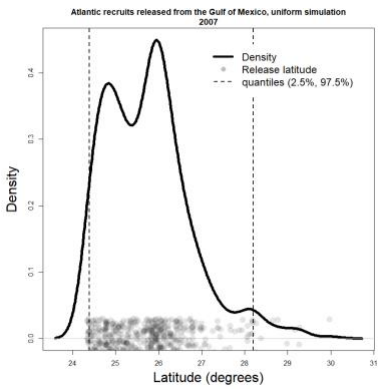
Atlantic recruits released from the Gulf of Mexico, uniform simulation
2007
Density
Release latitude
quantiles (2.5%, 97.5%)
Density
Latitude (degrees)

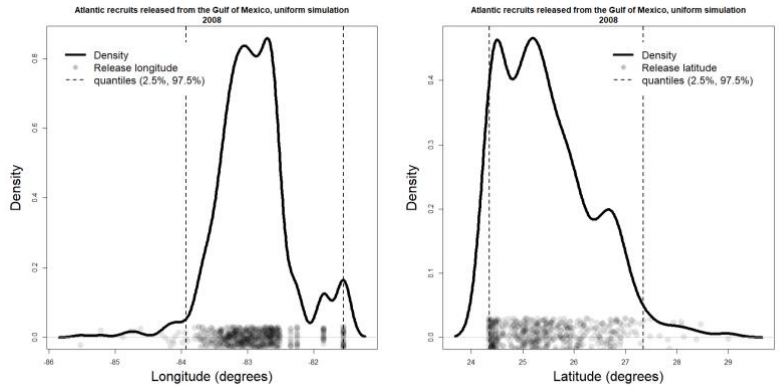

Figure S12. Density plots of longitude and latitude of the release locations of particles that were released in the Gulf of Mexico and settled in the Atlantic Ocean; individual years of the uniform particle release simulation.

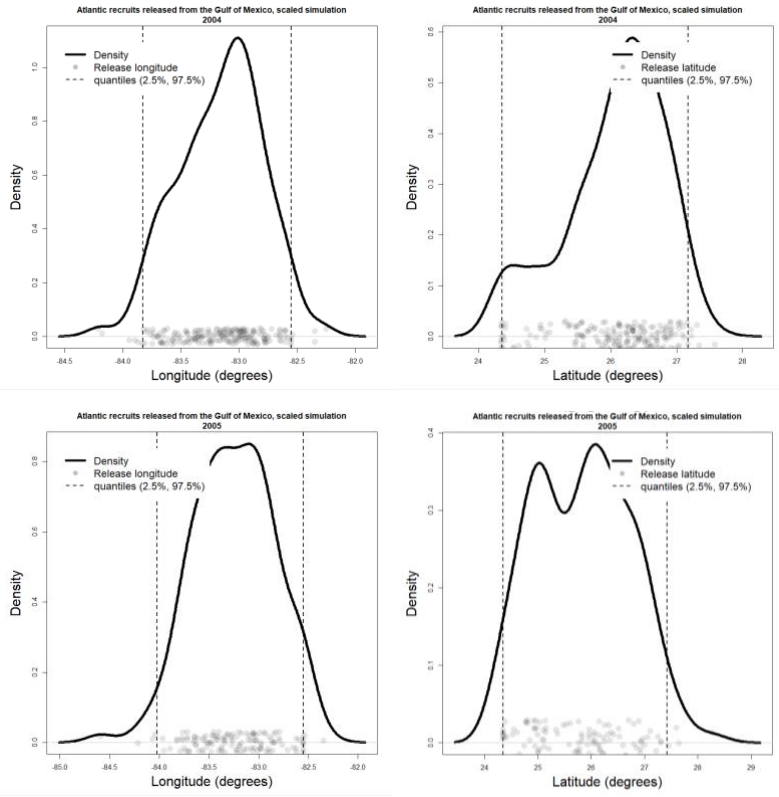

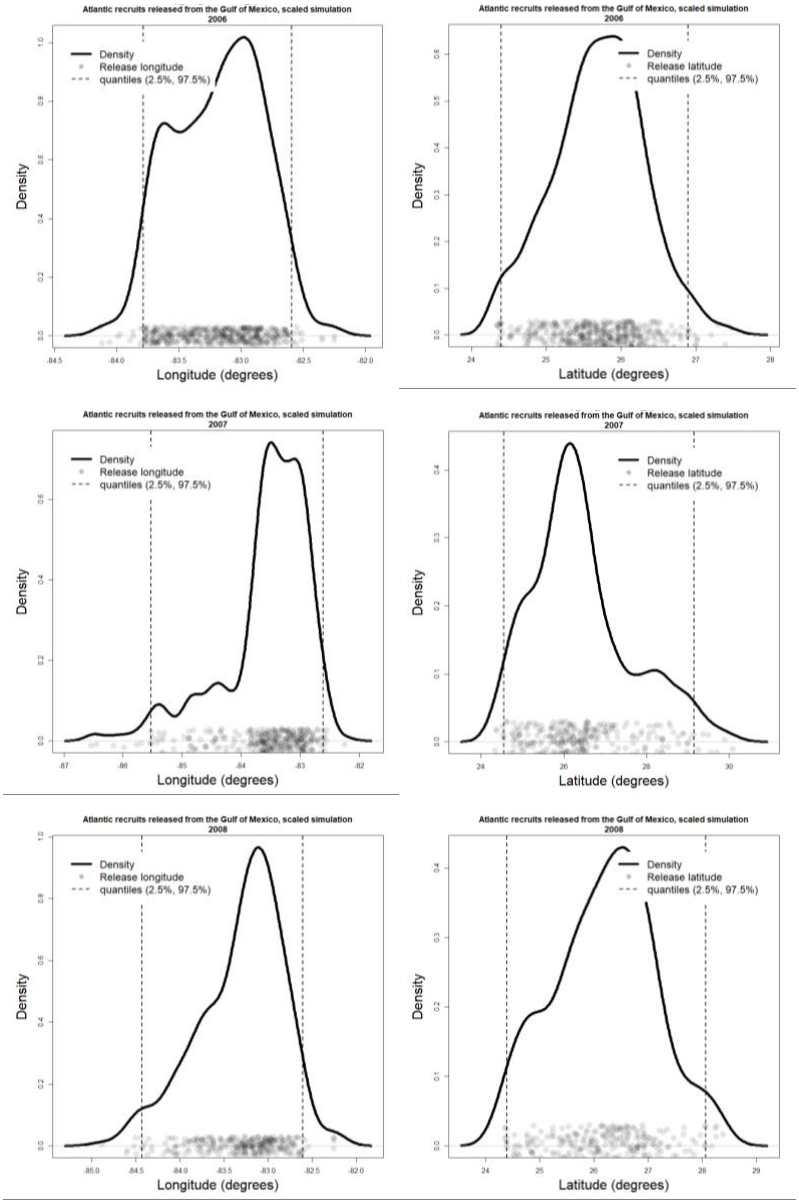

Figure S13. Density plots of longitude and latitude of the release locations of particles that were released in the Gulf of Mexico and settled in the Atlantic Ocean; individual years of the scaled particle release simulation.